Selective Sensing of Phosphorylated Peptides and Monitoring Kinase and Phosphatase Activity with a Supramolecular Tandem Assay

Yang Liu,[2] Jiwon Lee,[1] Lizeth Perez,[1] Adam D. Gill,[3] Richard J. Hooley[1,3]* and Wenwan Zhong[1, 2]*

[1]Department of Chemistry; [2]Environmental Toxicology Program; [3]Department of Biochemistry and Molecular Biology; University of California-Riverside, Riverside, CA 92521, U.S.A.

Supporting Information Placeholder

ABSTRACT: Simple tuning of a host: guest pair allows selective sensing of different peptide modifications, exploiting orthogonal recognition mechanisms. Excellent selectivity for either lysine trimethylations or alcohol phosphorylations is possible by simply varying the fluorophore guest. The phosphorylation sensor can be modulated by the presence of small (μM) concentrations of metal ions, allowing array-based sensing. Phosphorylation at serine, threonine and tyrosine can be selectively sensed *via* discriminant analysis. The phosphopeptide sensing is effective in the presence of small molecule phosphates such as ATP, which in turn enables the sensor to be employed in continuous optical assays of both serine kinase and tyrosine phosphatase activity. The activity of multiple different kinases can be monitored, and the sensor is capable of detecting the phosphorylation of peptides containing multiple different modifications, including lysine methylations and acetylation. A single deep cavitand can be used as a "one size fits all" sensor that can selectively detect multiple different modifications to oligopeptides, as well as monitoring the function of their PTM writer and eraser enzymes in complex systems.

INTRODUCTION

Protein post-translational modifications (PTMs) are key components of cellular regulation.[1] Histone modifications can include methylation, numerous different acylations, phosphorylation, and glycosylation, among others.[2] These important epigenetic mechanisms can induce changes in genome function without changing the underlying DNA sequence.[3] Their importance in cellular processes has led to a variety of investigations into their identification, function and creation/removal. There are many facets to this research: identification of the nature and location of new PTMs,[4] monitoring the modification process itself, which involves assays of PTM writer/eraser enzymes and their cooperativity,[5] and study of their downstream effects on cellular function.[6] Studying these different facets requires multiple techniques: mass spectrometry is the predominant technique for identifying peptide PTMs,[7] but becomes operationally challenging when applied to enzyme assays, in which high reproducibility and accurate quantitation are crucial. Antibodies have been employed to modified proteins or peptides with high specificity, [8] but they are expensive to obtain, must be expressed for each individual peptide, and require rigorous controls to ensure purity and reproducibility.[9] In addition, different techniques are needed for analysis of intact modified proteins, as opposed to peptide fragments and neither MS or antibody assays are capable of continuous analysis.

Small molecule optical sensors have recently gained prominence in detecting modifications on peptide chains,[10] and in supramolecular tandem assays of enzyme function.[11] They are often cheap, simple to use, and amenable to high throughput screening. Site-selective sensing is possible by employing "chemical nose" systems: arrayed small molecule sensors can provide site-selective recognition of modified peptides upon statistical analysis of the multivariant responses.[12] The limitations of sensing with synthetic receptors are that each individual molecule is tailored for a single modification type, and certain PTMs are more accessible than others. Calixarenes (CX) are excellent hosts and sensors for methylated lysine[13] residues, and cyclophanes can recognize both methylated lysines and arginines.[14] Neither of these hosts binds lysine acylations or serine phosphorylations, however. Similarly, cucurbiturils (CB) are good hosts for ammonium ions and N-terminal phenylalanine,[15] but have no affinity for phosphate. There are a number of small molecules that bind the phosphate group[16] and phosphorylated peptides,[17] most often polyammonium ions or metal-ligand complexes.[18] These recognition motifs are highly effective and can be coupled with fluorescence outputs for phosphate sensing, and arrayed sensors allow good site-selectivity.[19]

As well as the recognition, structural analysis and sensing of peptide PTMs, synthetic receptors have been applied in supramolecular tandem assays of enzyme function.[20] These assays have great potential for analyzing PTM writer/eraser function, kinetics, dependence on structural modifications, and enzyme cooperativity. Cavity-based hosts such as CB7 or CX4 are effective in assaying certain types of enzymes,[20] including chromatin writers and erasers such as lysine methyltransferase and demethylase,[20c] but site-selective monitoring of these enzymatic processes

is still rare. In addition, theses cavity-based hosts are not effective for monitoring phosphorylation enzymes such as kinases or phosphatases. Small molecule tandem assays of kinase/phosphatase activity requires that the sensor be tolerant to other small molecule phosphate cofactors, such as ATP and cAMP. Discrimination between phosphorylated peptides and small molecule phosphates is challenging for small molecule phosphate sensors, as their design principles focus on the recognition of the phosphate group, rather than the peptide.[16] Sensors that are tailored to recognize the phosphate group are more likely to be interfered with by the exogenous cofactors, and selectivity becomes paramount in their design. The most effective solution is to use peptides *covalently modified* with a phosphorylation recognition motif.[19] This allows optical and fluorescence-based assays of tyrosine and serine kinases and phosphatases,[21] whereby peptide strands synthetically modified with fluorophores can detect the addition/removal of phosphate groups, often *via* FRET or aggregation-induced fluorescence. Creating a label-free sensor that detects phosphorylation of free peptides would enable more biologically relevant applications, but is far more challenging.[22]

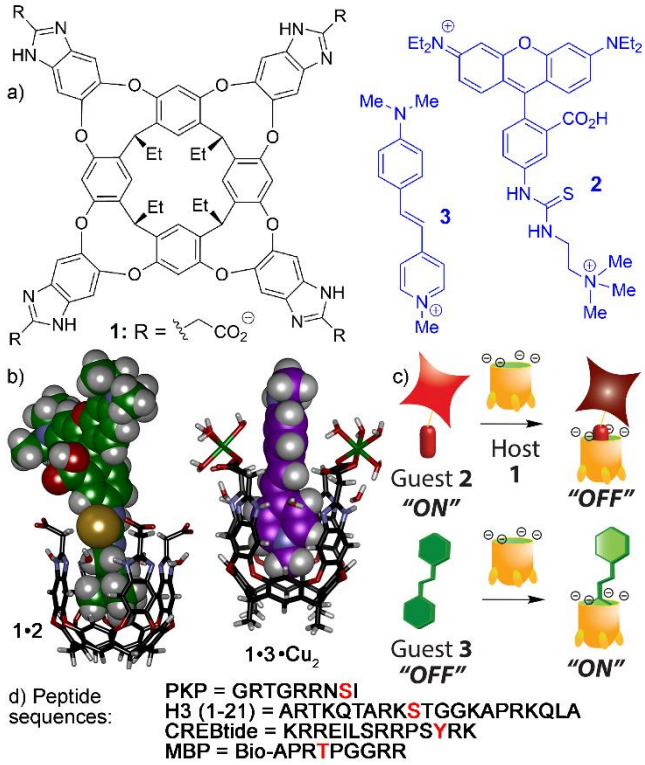

Figure 1. a) Structure of host **1** and guests **2, 3**; b) Minimized models of the **1•2** and **1•3•Cu$_2$** host:guest complexes (SPARTAN); c) Illustrations of the effects on emission intensity of binding fluorophores **2** and **3** in the cavity of **1**; d) peptide sequences used, red = residue of phosphorylation in the phosphorylated variant.

A "one size fits all" sensor system that can both detect different PTMs easily, with positional selectivity, and also be applied to supramolecular tandem assays of enzyme function would have multiple uses, and overcome some of the limitations of small molecule PTM sensors. We have recently shown that water-soluble deep cavitands such as **1**[23] (Figure 1) are capable of binding and sensing peptide PTMs *via* fluorescence displacement processes, and can be applied to site-selective sensing of lysine demethylases and methyltransferases.[24] The behavior of this host is quite complex, and it is sensitive to multiple different external factors, allowing different recognition mechanisms to occur with a single host molecule.[25] Here, we exploit these multiple recognition mechanisms, and create a sensing system that displays site-selective sensing of multiple different peptide PTMs show its applicability towards supramolecular tandem assays of both serine kinase and alkaline phosphatase function. Most interestingly, the assay is able to reveal the influence of nearby modifications on kinase activity.

RESULTS AND DISCUSSION

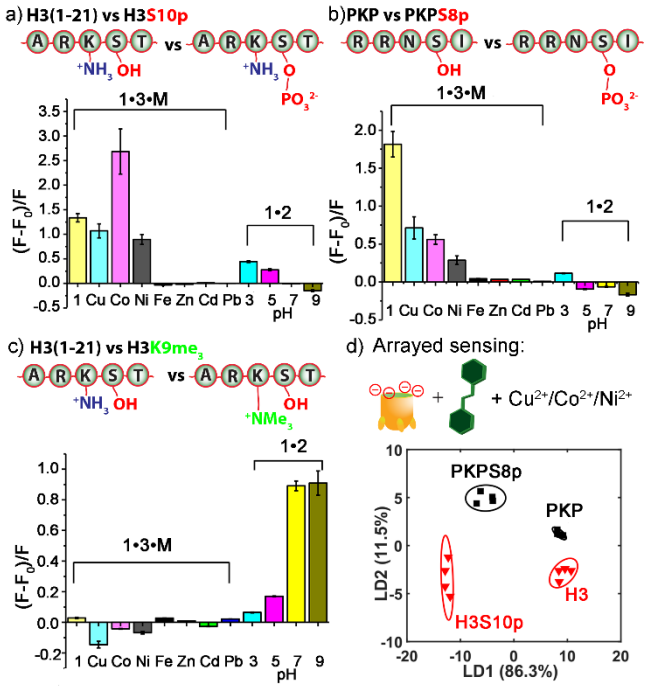

Figure 2. Relative fluorescence response of a) H3S10p; b) PKPS8p; c) H3K9Me$_3$ to their unmodified counterparts. F = response with modified peptide, F$_o$ = response with unmodified peptide.**1** = cavitand **1** with no metal additive. d) LDA scores plot with a 4-component array consisting of **1•3**, **1•3•Cu^{2+}**, **1•3•Co^{2+}** and **1•3•Ni^{2+}**. [peptide] = 10 μM. **1•3•M^{2+}**: [**1**] = 20 μM, [**3**] = 1.5 μM, [**M^{2+}**] = 10 μM, 20 mM Tris, pH 7.4. **1•2**: [**1**] = 3 μM, [**2**] = 4 μM, [**M^{2+}**] = 10 μM.

The internal cavity of host **1** is reminiscent of the acetylcholinesterase active site, and as such **1** has micromolar affinity for choline[23b] and trimethyllysine (Kme$_3$) residues.[24] This cavity-based recognition allows site-selective sensing of lysine methylations *via* a fluorescence displacement mechanism, using cholamine-derived fluorophores such as **2**, which are strong guests for **1** (K$_d$(**1•2**) = 1.51 μM at pH 7.4[24b]). Only Kme$_3$ groups bind strongly enough to effect displacement of the strongly bound **2**, conferring excellent pan-specificity for this modification. The host is also capable of binding other fluorophores such as DSMI **3**, albeit more weakly than **2** (K$_d$ (**1•3**) = 23.1 μM). Whereas **2** is

quenched upon binding, **3** is a turn-on fluorophore, and its emission is enhanced upon binding in the cavity of **1**.[25] The initial application of the **1•3** system was to sense heavy metal ions: the carboxylate groups in **1** are perfectly positioned to rotate and bind heavy metal ions in a chelated fashion, with affinities of up to K_d = 700 nM in aqueous solution.[25] These investigations showed multiple different mechanisms of fluorescence quenching and enhancement were involved, depending on the nature of the fluorophore and the metal. The exquisite sensitivity of the host to small concentrations of heavy metals and other external factors such as anions and pH[24a] suggested that employing **1•3** and different metal additives would allow detection of peptide PTMs that display changes in charge/H-bonding, as opposed to the standard cavity-based recognition process.

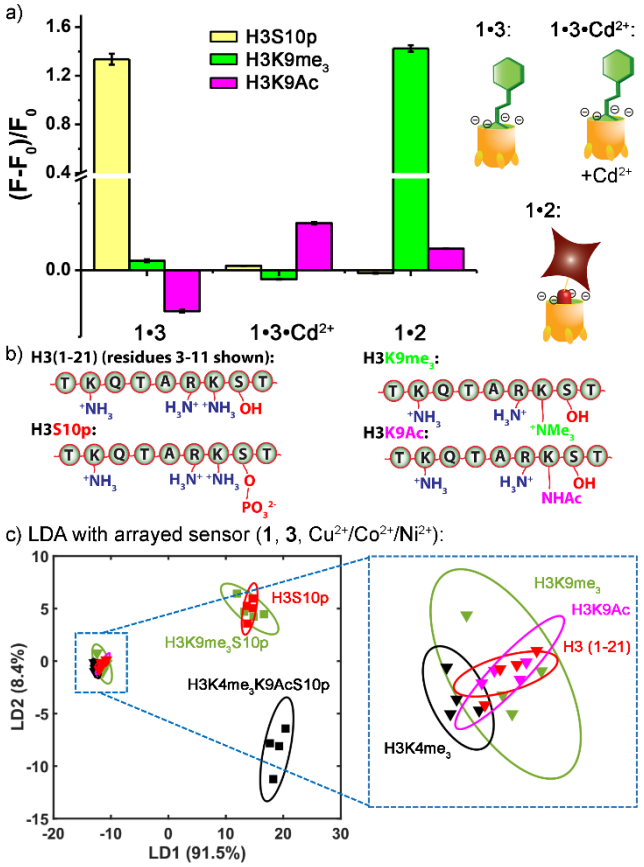

Figure 3. a) Comparison of individual sensor component responses to different PTM types. F = response with modified peptide, F_o = response with H3(1-21). [peptide] = 10 μM. **1•3•M²⁺**: [**1**] = 20 μM, [**3**] = 1.5 μM, [M^{2+}] = 10 μM, 20 mM Tris, pH 7.4. **1•2**: [**1**] = 3 μM, [**2**] = 4 μM, [M^{2+}] = 10 μM. b) Different peptide structures used. c) LDA scores plot of the selective phosphate sensing with a 4-component array consisting of **1•3**, **1•3•Cu²⁺**, **1•3•Co²⁺** and **1•3•Ni²⁺**.

The initial tests focused on the modification that conveyed the largest change in charge/H-bonding to the peptide, serine phosphorylations. Solutions of either **1•3•M²⁺** ([**1**/**3**/M] = 20/1.5/10 μM) with various metal salts at pH 7.4, or **1•2** in varying pH buffers ([**1**/**2**] = 3/4 μM) were exposed to 10 μM peptide strands containing phosphorylated serine residues. Two different phosphorylated peptides were tested, a 21-amino acid histone H3 peptide (H3 1-21, ARTKQTARKSTGGKAPRKQLA) phosphorylated at serine 10 and a nine amino acid substrate for protein kinase A (PKP) phosphorylated at serine 8 (GRTGRRNSI, Figure 1d). As can be seen in Figure 2 (raw fluorescence plots shown in Supporting Information), the **1•3•M²⁺** complexes showed variable enhancement in fluorescence (F) in the presence of 10 μM phosphorylated peptide, when compared to the emission (F_o) in the presence of the non-phosphorylated counterpart. The enhancement does not require the presence of metal salts, as the fluorescence of **1•3** is enhanced by both H3S10p and PKPS8p. Addition of 10 μM of a series of transition metals had variable effects on the sensing process: metals that strongly quench **1•3**,[25] such as Cu^{2+}, Co^{2+}, and Ni^{2+} gave differential, variable enhancements in signal for the two different peptides. In contrast, no differentiation between H3 and H3S10p was observed for **1•3** in the presence of 10 μM Fe^{3+}/Zn^{2+}/Cd^{2+} or Pb^{2+}. Most importantly, the Kme_3-selective fluorophore **2** was only minimally affected by the presence of serine phosphate PTMs. The **1•2** sensor showed minimal distinction between the peptides, as neither the phosphorylated nor the unmodified peptide is capable of displacing the guest from the cavitand. Whereas the **1•2** host:guest complex shows a strong response to trimethylated lysine peptides (Figure 2c), the **1•3•M²⁺** sensors showed no distinction between unmodified H3 and H3Kme_3. Simple variation of the guest fluorophore allows orthogonal selectivity in target sensing.

The differential responses in the presence of metal ions allow the **1•3•M²⁺** host:guest sensors to be applied in array-based format for more selective discrimination between phosphorylated substrates. When four sensor elements (**1•3**, **1•3•Cu²⁺**, **1•3•Co²⁺** and **1•3•Ni²⁺**) are combined into an array, and the fluorescence responses subjected to linear discriminant analysis (LDA),[26] the phosphorylated peptides are well separated from their unmodified counterparts on the scores plot (Figure 2d). All three repeats were included in the 95% confidence ellipses with no overlap among different peptides. The H3/H3S10p pair exhibited greater separation distance than the PKP/PKPS8p pair, due to the larger fluorescence change they induced in all 4 sensor elements.

The initial tests illustrate the capabilities of the host:guest sensor system: by simply varying the nature of the fluorescent guest, the system can be tailored to detect different types of peptide modification, while keeping the cavitand constant. The **1•2** sensor can selectively detect lysine trimethylation,[24b] but is ineffective in sensing phosphorylation. The **1•3** sensor (either with or without the presence of Cu^{2+}, Co^{2+} or Ni^{2+}) does not show any difference in emission in the presence of Kme_3, but is an effective phosphorylation sensor. The sensitivity of the **1•3** sensor can be exploited to favor detection of other types of peptide PTM. Interestingly, in the presence of 10 μM Fe^{3+}/Zn^{2+}/Cd^{2+} or Pb^{2+}, the **1•3** sensor responded to neither Kme_3 nor S1op, but showed up to 15% emission enhancement for lysine acetylation (KAc), with the largest fluorescence increase observed for **1•3•Cd²⁺** and **1•3•Pb²⁺** (Supporting Information). Figure 3a summarizes these observa-

tions: by simply varying the additives combined with cavitand **1**, the system can favor selective detection of either lysine trimethylation ($H3K9me_3$, with **1•2**) serine phosphorylation (H3S10p, with **1•3**) or lysine acetylation (H3K9Ac, with **1•3•Cd**$^{2+}$). Each of the sensor elements was only minimally affected by the non-matched modifications.

The selectivity of the **1•3** sensor for phosphorylation PTMs is such that it is capable of detecting phosphorylations on peptides that carry other types of PTMs as well (Figure 3c). The four-component phosphorylation-sensitive array consisting of **1•3**, **1•3•Cu**$^{2+}$, **1•3•Co**$^{2+}$ and **1•3•Ni**$^{2+}$ (hereinafter described as **1•3•M**$^{2+}$) was used to compare the fluorescence responses from H3S10p, $H3K4Me_3K9AcS10p$ and $H3K9Me_3S10p$ to those from H3 (1-21), H3K9Ac, $H3K4Me_3$ and $H3K9Me_3$. As expected, the **1•3•M**$^{2+}$ array was unable to distinguish between the non-phosphorylated peptides H3 (1-21), H3K9Ac, $H3K4Me_3$ and $H3K9Me_3$, as they all colocalized on the LDA scores plot. Excellent discrimination was possible between the four non-phosphorylated peptides and the H3S10p peptides, however. Each of H3S10p, $H3K4Me_3K9AcS10p$ and $H3K9Me_3S10p$ could be discriminated from the non-phosphorylated equivalents. Impressively, the simple four component **1•3•M**$^{2+}$ array was capable of distinguishing between H3S10p and $H3K4Me_3K9AcS10p$, indicating that the sensor is not only selective for phosphate PTMs, but can display selectivity between multiply modified peptides as well.

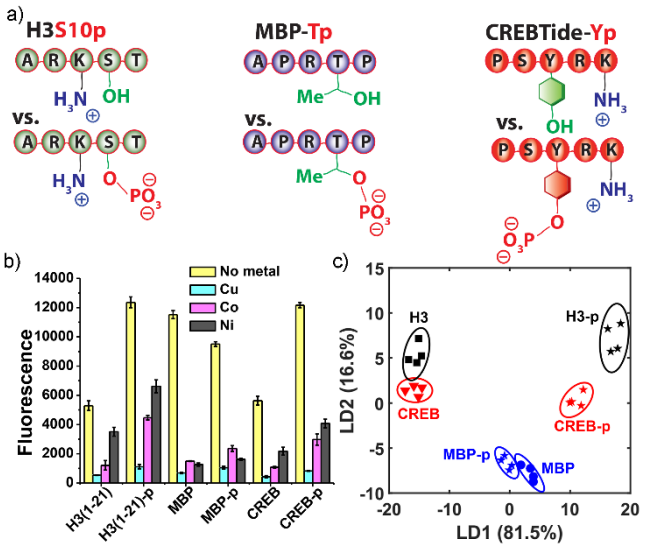

Figure 4. a) Peptide substrates phosphorylated at different alcoholic residues; b) raw fluorescence response and c) LDA scores plot of phosphorylated peptides and their unmodified counterparts with a 4-component array consisting of **1•3**, **1•3•Cu**$^{2+}$, **1•3•Co**$^{2+}$ and **1•3•Ni**$^{2+}$.

As the **1•3•M**$^{2+}$ array showed the greatest selectivity for the presence of phosphorylations, we tested its ability to detect the addition of phosphate PTMs on the other commonly modified residues, tyrosine (Y) and threonine (T). The **1•3•Cu/Co/Ni**$^{2+}$ sensor array was added to 10 μM solutions of peptides containing either Y or T phosphorylation (Figure 4a, CREBTide and MBP, respectively, for full sequences see Figure 1d) and their unmodified counterparts. The fluorescence pattern from CREBtide-Yp is quite similar to that of H3S10p, with the tyrosine-phosphorylated peptide showing a 2-3 fold increase in fluorescence in all four sensor components (Figure 4b). The fluorescence changes induced by T phosphorylation on MBP were smaller than the S or Y phosphorylated peptides, but performing LDA on the fluorescence profiles results in clear separation of the three phosphorylated peptides (Figure 4b). In each case, the phosphorylated and non-phosphorylated forms were clearly separated with minimum overlap of the 95% confidence ellipses. This indicates that the array is capable of acting as a selective, yet "pan-specific" sensor for phosphorylation on multiple potential amino acid substrates.

The orthogonal selectivity of the two different host:guest sensors, as well as their pan-specificity for the target modifications, suggests that the sensing processes occur *via* different mechanisms for each fluorophore guest. The mechanism of the Kme_3 detection process with guest **2** is simple: guest **2** is quenched upon binding in **1**, and only the strongly binding Kme_3 group can cause displacement and fluorescence recovery.[24b] The fluorescence response of the **1•2** complex is unaffected by the presence of unmethylated cationic peptides, as the **1•2** affinity is so high:[24b] any interaction between the negatively charged host **1** and cationic oligopeptides does not cause displacement of **2**. However, we have previously observed that anionic host **1** does have a strong binding affinity for cationic peptides, a phenomenon that could be detected when more weakly bound fluorophores were used.[24a] This affinity could be modulated by Hofmeister effects under high salt conditions, and is the most likely explanation for the selective phosphorylation sensing with **1•3**. To further elucidate this process, we investigated the interaction of cavitand **1** with peptide substrates *via* isothermal calorimetry (ITC, Figure 5, Table 1 and Supporting Information).

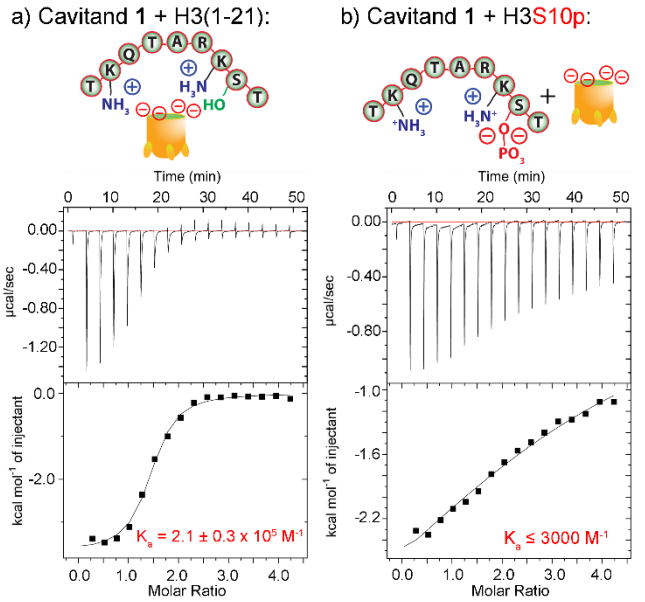

Figure 5. ITC measurements showing the affinity of **1** for a) H3(1-21) and b) H3S10p. [peptide] = 100 μM, 20 mM Tris,

pH 7.4, 25 °C. Each injection: 2.43 µL of a 2 mM solution of **1**.

Table 1. Thermodynamic data (ITC) for the interactions of **1** with peptide targets.

Peptide	K_a(**1**), x 10^5 M^{-1}	ΔH, kcal mol^{-1}	ΔS, cal/mol/K
H3	2.11 ± 0.3	-3.7	+12
PKP	2.68 ± 0.5	-4.4	+10
MBP	0.30 ± 0.04	-4.9	+4
H3S10p	<0.03	n.d.	n.d.
MBP-T97p	N/A	N/A	N/A

Five peptides were tested for their affinity to cavitand **1**: three cationic peptides (H3(1-21), PKP and MBP), as well as two phosphorylated peptides (H3S10p and MBP-p). Cavitand **1** showed strong affinity for each of the unmodified cationic peptides, ranging from 2.68 x 10^5 M^{-1} (PKP) to 0.30 x 10^5 M^{-1} (MBP). In each case, binding event is both enthalpically and entropically favored, suggesting that both H-bonding/charge interactions and a favorable desolvation of the cavitand exterior occurs upon binding. Interestingly, the n values vary from n = 1.39 (H3) to n = 0.67 (PKP), depending on the peptide length, suggesting variable valency in the binding event. As cavitand **1** only shows affinity for oligopeptides, and not for free amino acids or products of protein digests,[24a] this makes sense: the **1**•peptide coordination must involve multiple points of contact and H-bonds, as well as charge matching, and multiple cavitands could be able to bind the peptide backbones. In contrast, the two phosphorylated peptides showed much lower affinity. In both cases, full binding was challenging to attain by ITC, indicating binding affinity was on the order of millimolar or lower. Estimated fitting for the binding of H3S10p is ≤ 3,000 M^{-1}, which is at least 70 times smaller than its non-phosphorylated counterpart (Figure 5b), whereas the affinity for the phosphorylated short peptide MBP-p could not be measured, as it was significantly below the limit of detection of the ITC experiment (Supporting Information).

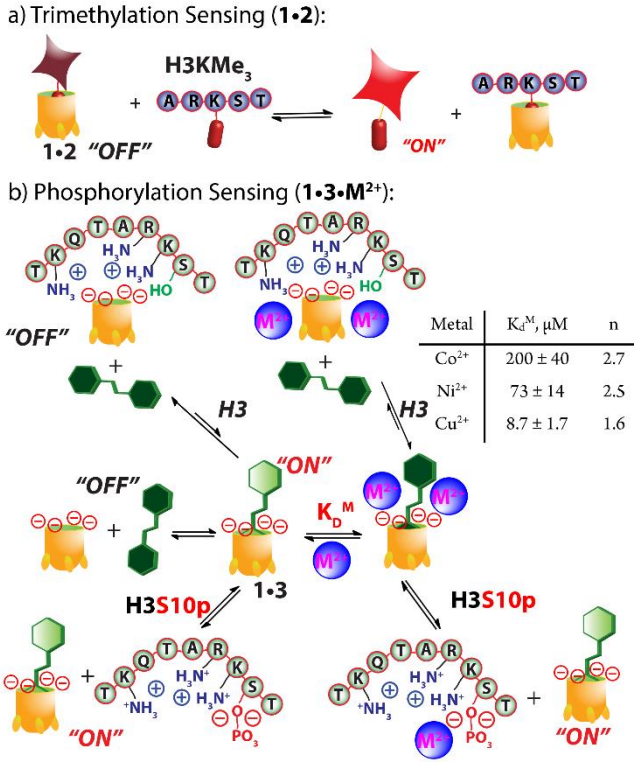

Figure 6. Equilibria present in the **1•3** phosphopeptide sensing mechanism. [**1**] = 20 µM, [**3**] = 1.5 µM, pH 7.4, 20 mM Tris. K_d^M determined *via* Hill equation.[25,27]

This wide variation in binding between host **1** and cationic/phosphorylated peptides sheds light on the mechanism of sensing by the **1•3** sensor. Evidently, the binding between **1•3** and the peptide targets affects the emission of the **1•3** complex, unlike the more strongly bound **1•2**. The more weakly bound guest **3** is likely expunged upon the charge-mediated **1•peptide** interaction (see Figure 6). As **3** protrudes from the top of the host, any interaction between peptide ammonium ions and the upper rim carboxylates of **1** will sterically interfere with the **1•3** binding event. This expulsion removes the fluorescence enhancement seen from the **1•3** complex. In contrast, when **1•3** is added to a *phosphorylated* peptide, the affinity is lower. Introduction of phosphate groups to the cationic peptide lowers the overall isoelectric point (pI), which lowers the affinity for **1**, increasing the [**1•3**] in the system and concomitantly increasing the fluorescence signal. This mechanism of sensing is important - as the recognition event is between **1•3** and the cationic peptide, *not the phosphate group itself*, the sensing is not affected by the presence of small molecule phosphates such as 50 µM ATP or cAMP, 50 mM phosphate buffer. Addition of 500 µM ATP causes a 27% increase in signal (see Supporting Information), far less than the 170% increase with 10 µM PKPS8p, for example.

There are other facets of the sensing mechanism that are unusual, namely the effect of metal additives and the fact that the **1•3•M**$^{2+}$ complex shows no response to Kme_3 peptides. The lack of response to Kme_3 of the **1•3** sensors is easily explained: the optimal concentration of **1** for enhanced fluorescence of **3** is 20 µM (to 1.5 µM **3**). The affinity of 23 µM for **1•3** corresponds to a bound ratio ~50% for **3** at the

concentrations used here. Unoccupied **1** will bind any Kme_3 peptides present, but at [peptide] = 10 μM, this has minimal effect on the **1•3** signal enhancement.

The effect of Cu/Co/Ni^{2+} on the response of **1•3** for phosphorylated peptides is more complex, and possibilities are laid out in Figure 6b. In the presence of metal ions, there are three **1•3•M**$^{2+}$ states that contribute to the emission intensity of **3**: free **3**, the **1•3** complex, and the ternary **1•3•M**$^{2+}$ complex. As described in detail in our previous publications,[25, 28] the sensing and coordination of **1** to fluorophores and metal ions is complex, and depends greatly on the nature of the metal and fluorophore. Fortunately, the three metal ions that were successful in modulating the fluorescence of **1•3** with phosphorylated peptides (i.e. Cu^{2+}, Co^{2+}, Ni^{2+}, Figure 2a,b) all behave the same way when added to **1•3**. All three metals have strong affinity for **1•3**, but the K_d values are quite variable, ranging from 8.7±1.7 μM (Cu^{2+}) to 200 ± 40 μM (Co^{2+}). These values were obtained by fitting to the Hill equation,[27] with *no displacement of guest* **3**. No fit was obtained to a model that incorporated dissociation of the **1•3** complex for these three metals,[25,29] indicating that the **1•3** complex remains *intact* after binding Cu^{2+}, Co^{2+}, Ni^{2+}. This is in contrast to other heavy metals (e.g. Ce^{3+} or Pb^{2+}) which showed strong affinity to **1**, but caused significant dissociation of **1•3** in the process.[25] Those metals were unsuccessful in modulating the fluorescence of **1•3** with phosphorylated peptides, however, so we need not consider these more complex mechanistic possibilities here. For a fuller discussion, please see reference 25.

When complexed, all three metals (Cu^{2+}, Co^{2+}, Ni^{2+}) cause significant quenching of **1•3** by the heavy atom effect.[28] The quenching amount is relatively consistent once fully bound: the major variable between each is its affinity of the metal for the **1•3** complex. Addition of metals will affect the affinity of **1•3** for the peptide/phosphopeptide (presumably enhancing the affinity for phosphopeptide *via* charge matching), as well as the emission of **3** when bound to the host. Variable affinities of **M**$^{2+}$ for **1•3** lead to varying concentrations (and emission intensities) of each component shown in Figure 6. The large number of equilibria precludes accurate quantitation of the effect on peptide binding in these cases. However, the qualitative effect is clear: addition of different metals is an effective method of introducing variables in the sensor array that allow simple, robust discriminant analysis between both peptides and their phosphorylated counterparts, as well as between peptides phosphorylated at different residues.

The selectivity of **1•3** for phosphopeptides and its tolerance to small molecule phosphates suggested that this would be a good candidate for monitoring enzymatic peptide phosphorylation/dephosphorylation in a supramolecular tandem assay. Phosphorylation is mediated by PTM writers that add phosphate to peptides (i.e. kinases), and erasers that remove phosphates (i.e. phosphatases).[30] For effective enzyme monitoring, the sensor must be tolerant to the cofactors required for enzymatic reaction. Kinases require the presence of two different phosphate-containing species (ATP and cAMP), plus a divalent metal cation, Mg^{2+}. As the **1•3** sensor shows no affinity for small phosphates, and is mediated by the nature of the cationic peptide, it is well-suited for this task. Notably, Mg^{2+} causes no change in the fluorescence of **1•3**,[25] so does not interfere in the sensing. We applied the **1•3** sensor to continuous monitoring of the phosphorylation of serine 10 in H3 (1-21) by protein kinase A.[31] The sensor was added to the enzyme reaction mixture (containing 0.01 mg/mL PKA, 20 μM ATP, 0.1 mM Mg^{2+}, 5 μM cAMP, in 100 μL 20 mM Tris buffer at pH 7.4) from time zero, and the reaction was monitored in a plate reader every 10 mins. As the phosphorylation progressed, the fluorescence increased as expected, and faster reaction rates were observed at higher [peptide] within the range of 0 – 10 μM. The reaction with 10 μM peptide was also monitored by removing aliquots from the reaction, inactivating the enzyme and subjecting the samples to MALDI-MS analysis. The product/total (product + substrate) ratio determined by MS matches well with the ratio determined from the **1•3** fluorescence response (Figure 7a). This rate corresponds well to the known activity of the enzyme. At t = 100 min, 50% of the H3 peptide, i.e. 50 pmol, was phosphorylated, and 1 μg enzyme should transfer 0.5 picomoles of phosphate per minute.

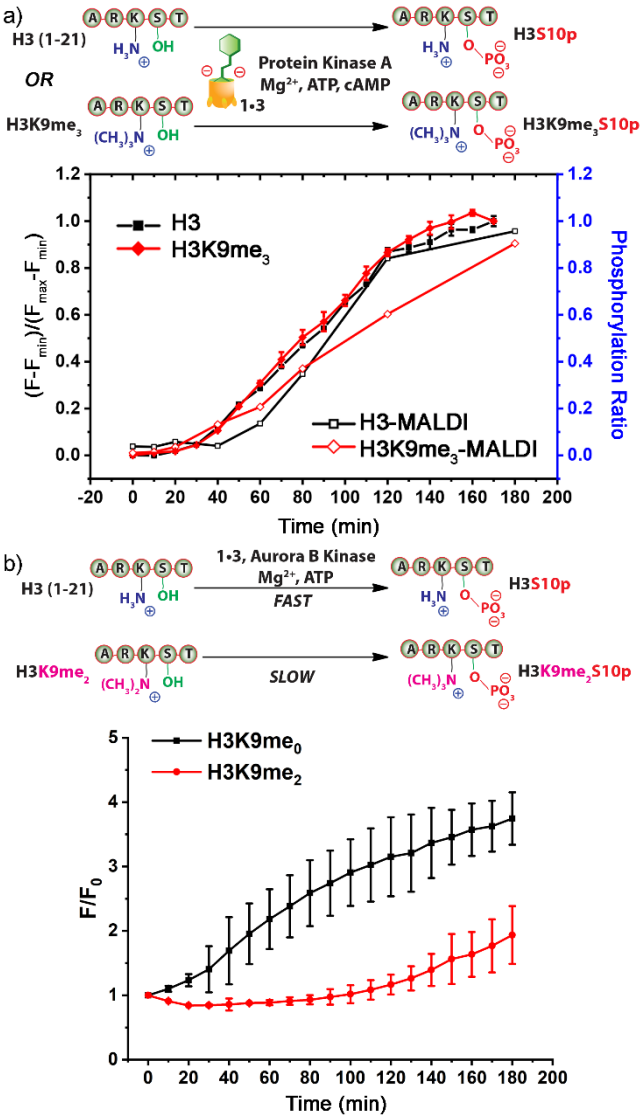

Figure 7. a) Comparison of fluorescence response of **1•3** and MALDI analysis of the phosphorylation of H3 (1-21) and $H3K9me_3$ by the unselective Protein Kinase A at 0.01 mg/mL. b) Comparison of fluorescence response of **1•3** upon the phosphorylation of H3 (1-21) and $H3K9me_2$ by the methylation-selective Aurora B Kinase at 0.005 mg/mL. Both enzyme reactions also contained 0.1 mM Mg^{2+}, 20 μM ATP, 0 (for Aurora B) or 5 (for PKA) μM cAMP, 10 μM peptide, 20 mM Tris, pH 7.4; as well as the sensor: [**1**] = 20 μM, [**3**] = 1.5 μM.

To further illustrate the power of the **1•3** sensor system we tested its efficacy in monitoring kinase activity. We first tested PKA-catalyzed S10 phosphorylation on H3 (1-21) peptides carrying $K9me_3$ (Figure 7a) or K9Ac (Supporting Information). The presence of $K9me_3$ or K9Ac groups does not appreciably affect the rate of S10 phosphorylation by PKA as shown by MALDI-MS analysis of the reaction progress. Excitingly, the **1•3** sensor was fully effective in monitoring the progress of phosphorylation in both of these cases, despite the fact that one of the peptides carries a lysine trimethylation modification.

Furthermore, we evaluated the capability of our sensor in monitoring a kinase that is differentially selective for peptides carrying different modifications. Aurora B Kinase is known to phosphorylate serine residues in peptides carrying adjacent Kme_2 modifications more slowly than the unmodified lysine counterpart.[32] This provides a stringent test for the sensor: not only must it be effective in sensing the phosphorylation process, it must be able to differentiate between reactions occurring at different rates. As before, the sensor was added to the enzyme reaction mixture (containing 0.005 mg/mL Aurora B Kinase, 20 μM ATP, 0.1 mM Mg^{2+}, in 100 μL 20 mM Tris buffer at pH 7.4) from time zero, and the reaction progress was monitored in a plate reader every 10 mins for two peptides, H3 (1-21) and $H3K9me_2$. The fluorescence responses (Figure 7b) clearly show the different rates of Aurora B Kinase to the different peptides: the greatest enhancement in fluorescence is observed for the peptide that was phosphorylated fastest (H3), and the response with the less reactive peptide ($H3K9me_2$) was concomitantly lower. The reaction was also monitored by MALDI-MS (Supporting Information), and similar response curves were obtained. This shows that the **1•3** sensor is an effective monitor of multiple different kinases, *via* a continuous optical assay process that is tolerant to exogenous small molecule phosphate cofactors and capable of function in the presence of other, non-phosphorylation PTMs, including multiple lysine methylations and acetylation. In addition, the ability to detect differential kinase activity on different peptide substrates illustrates the capability of our sensor in helping study how various PTM enzymes collaborate in the regulation of protein functions.[33] The sensor is continuous and does not require waiting for full equilibration before each detection: we took measurements every 10 mins, but more data points can easily be collected. The major disadvantage we found to this method is at very low concentrations, as can be seen by the lag in detection in Figure 7a. Only after 10 mins did sufficient reaction occur to be detected, but we believe this is only as minor drawback, as out tested enzyme and peptide concentrations are relatively low in all cases.

Finally, we tested whether **1•3** sensor was also capable of monitoring phosphate removal with alkaline phosphatase (Figure 8). As the targets for tyrosine alkaline phosphatase are similar to those of the kinases, the process should be equally effective, with the only variation being a loss in fluorescence of **1•3** as the phosphorylated peptide is consumed, rather than created. Alkaline phosphatase does not require ATP and cAMP as cofactors, so the reaction is simpler than the corresponding kinase reaction. The **1•3** sensor was added to the reaction containing 10 μM CREBtide and 0-5 U/mL alkaline phosphatase in 20 mM Tris (pH 7.4) and the reaction monitored over time as before. In this case, the sensor fluorescence decreased over time as the proportion of phosphorylated peptide decreased, and the proportions matched the results from MALDI measurement of the same enzyme mixture (see Supporting Information). The sensor was capable of detecting rate differences upon varying the concentration of enzyme (Figure 8), and varying the peptide concentration allowed calculation of the Michaelis–Menten constant K_m for Crebtide-Yp dephosphorylation (Supporting Information).

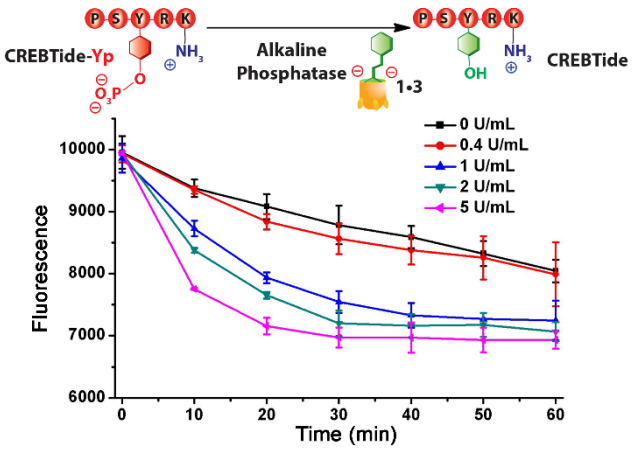

Figure 8. Assay of alkaline phosphatase activity on CREBtide-Yp using the **1•3** sensor with varying [enzyme]. [peptide] = 10 μM, [**1**] = 20 μM, [**3**] = 1.5 μM, 20 mM Tris, pH 7.4.

CONCLUSIONS

In conclusion, we have demonstrated that simple tuning of a deep cavitand:fluorophore guest pair allows selective sensing of different peptide modifications, exploiting orthogonal recognition mechanisms for the selectivity. Despite the fact that the host is unchanged, excellent selectivity for either lysine trimethylations or alcohol phosphorylations is possible by varying the fluorophore. The phosphorylation sensor can be modulated by the presence of small (μM) concentrations of metal ions, allowing array-based sensing and discrimination of phosphorylated peptides that vary by the presence of other PTMs, or by the residue of phosphorylations. Phosphorylation at serine, threonine and tyrosine can be both detected and the different peptides discriminated by discriminant analysis. The mechanism of phosphorylation sensing is controlled by the affinity of the host for cationic peptides, and the lower affinity upon addition of the anionic phosphate group. This mechanism allows the sensing to be effective in the presence of small molecule phosphates such as ATP, which in turn enables the sensor to be employed in kinase and phosphatase assays that use ATP as cofactor. The activity of multiple different kinases can be monitored, and the sensor is capable of function in the presence of other, non-phosphorylation PTMs, including multiple lysine methylations and acetylation. In addition, the sensor is compatible with monitoring phosphorylation and dephosphorylation at different residues, including serine and tyrosine. A single deep cavitand is a "one size fits all" sensor: the simplicity, selectivity and easy tunability of the continuous optical assay process is a powerful tool for rapid analysis of PTM peptides, as well as their writer and eraser enzymes in complex systems.

EXPERIMENTAL SECTION

General Information. Cavitand **1**[23b] and guest **2**[24b] were synthesized and characterized according to literature procedures. ^{1}H and ^{13}C NMR spectra were recorded on a Varian Inova 300 MHz, 400 MHz NMR spectrometer, and Bruker 500 MHz NMR spectrometer. All NMR spectra were processed using MestReNova by Mestrelab Research S.L. Deuterated NMR solvents were obtained from Cambridge Isotope Laboratories, Inc., Andover, MA, and used without further purification. Mass spectra were recorded by electrospray ionization on an LTQ-XL linear ion trap mass spectrometer (Thermo Scientific, San Jose, CA). Solvents were dried through a commercial solvent purification system (Pure Process Technologies, Inc.). MALDI-MS spectra were obtained using an AB Sciex TOF/TOF 5800 MALDI mass spectrometer in the positive ion mode. Molecular modelling (semi-empirical calculations) was performed using the AM1 force field using SPARTAN. Fluorescence measurements were achieved in a Perkin Elmer Wallac 1420 Victor 2 Microplate Reader (PerkinElmer) with the Ex/Em wavelengths at 530/605 nm or 440/605 nm. All peptides except the Protein Kinase A substrate were purchased from Anaspec and used as received. Protein Kinase A from bovine heart and its peptide substrate, Alkaline Phosphatase, *trans*-4-[4-(dimethylamino)-styryl]-1-methyl-pyridinium iodide (DSMI), Aurora B kinase were purchased from Sigma Aldrich (St. Louis, MO). All other materials, including metal salts, ATP and cAMP were purchased from Sigma Aldrich (St. Louis, MO) or Fisher Scientific (Fairlawn, NJ), and were used as received. Linear Discriminant Analysis (LDA) was performed with RStudio (Version 1.0.136), an integrated development environment (IDE) for R (version 3.3.2). Confidence ellipses were drawn with the data obtained from PCA using Matlab (version R2016b) and a self-developed script.

Experimental Procedures

Fluorescence measurements. In general, the fluorescence assay was carried out by mixing 10 μL of the fluorescent guest **2** (30 μM) or **3** (15 μM), 10 μL of the cavitand **1** (40 μM for **2** and 200 μM for **3**), 10 μL metal salts (100 μM in water), 60 μL of the incubation buffer (Tris buffer HCl, pH 7.4, 20 mM) in the 96-well plate, adding 10 μL of the peptide solution at 100 μM to bring the total volume up to 100 μL, and incubating with mild shaking for 15 mins at room temperature. The fluorescence signal (F) was recorded in a Perkin Elmer Wallac 1420 Victor 2 Microplate Reader (PerkinElmer) with the Ex/Em wavelengths at 530/605 nm for guest **2** and 440/605 nm for guest **3**.

Preparation of phosphorylated peptide. Non-phosphorylated peptide substrates (a 21-amino acid histone H3 peptide (H3 1-21) and a nine-amino acid substrate for protein kinase A (PKP, GRTGRRNSI) were first dissolved in water with a concentration of 1 mg/mL. In a typical phosphorylation reaction, a final concentration of 1 mM Mg^{2+}, 200 μM ATP, 50 μM cAMP, 100 μM peptides were added sequentially into a 2 mL centrifuge tube, and Tris buffer (pH 7.4, 20 mM) was added to bring the volume to 900 μL; then, PKA (100 μL, 1 mg/mL) was added immediately to bring the total volume to 1 mL. The mixture was incubated overnight at room temperature. The reaction was stopped by heating the tube at 100 °C in water bath for 5 minutes. Successful phosphorylation was confirmed by MALDI (Figure S12). The product was used directly without further modification since other components within the reaction

mixture did not impact on the sensor fluorescence (Figure S13).

Kinase and alkaline phosphatase activity assay. Continuous monitoring of PKA catalyzed phosphorylation of H3 or PKP was performed by mixing 10 μL of enzyme reaction solution (1 mM Mg^{2+}, 200 μM ATP, 50 μM cAMP and 100 μM peptide), 10 μL of 15 μM guest **3**, 10 μL of 200 μM cavitand **1**, 60 μL Tris buffer (pH 7.4, 20 mM) and finally 10 μL of PKA at various concentrations. Similar process was used for monitoring the activity of Aurora B kinase, except that cAMP was not needed for this enzyme. The alkaline phosphatase assay was carried out by mixing 10 μL of 15 μM guest **3**, 10 μL of 200 μM cavitand **1**, 10 μL of 100 μM CREBtide, 60 μL Tris buffer (pH 7.4, 20 mM) and 10 μL of alkaline phosphatase at various concentrations. The fluorescence was recorded by the plate reader at every 5 min.

MALDI-TOF MS analysis. The enzymatic reaction was carried out as described above. Aliquots were taken out at various time points and heated to deactivate the enzyme. A saturated solution of α-cyano-4-hydroxycinnamic acid (CHCA) was prepared in a 1:1 mixture of pure acetonitrile and 0.1% formic acid, and used as the matrix. A mixture of 0.5 μL of the matrix and 0.5 μL of the reaction aliquot was spotted on a stainless steel Opti-TOF™ 96 targets plate, and allowed to dry completely before being introduced into the mass spectrometer. Analysis was carried out on an AB Sciex 5800 TOF/TOF proteomics analyzer with a laser irradiation at a repetition frequency of 1000 Hz. A laser intensity index of 2800 was used for sample ionization and the MS spectra were acquired in the positive reflector mode within the mass range from 500 to 3,000 Da.

ITC measurements. All ITC experiments were performed using a MicroCal iTC200 (GE Healthcare, Freiburg, Germany) with a stirring rate of 700 rpm. The baseline was stabilized prior to the experiment, and a pre-injection delay was set to 60 s. The first injection was 0.4 μL while the remaining injections were 2.43 μL, performed every 180s. The reference power was set to 5 μcal/sec. The syringe contained 2 mM negative cavitand while the cell contained 0.1 mM peptide. All experiments were conducted at 25 °C. Curve fitting was performed with Origin using the standard one site model provided by MicroCal. The standard one site model uses the following equation:

$$\Delta Q(i) = Q(i) + \frac{dV_i}{V_0}\left[\frac{Q(i)+Q(i-1)}{2}\right] - Q(i-1)$$

Where Q(i) = total heat content at the end of the ith injection, V_o = active cell volume.

ASSOCIATED CONTENT

Supporting Information

New molecule synthesis and characterization and additional spectral data. This material is available free of charge *via* the Internet at http://pubs.acs.org.

AUTHOR INFORMATION

Corresponding Authors

* E-mail: richard.hooley@ucr.edu; wenwan.zhong@ucr.edu

ACKNOWLEDGMENTS

The authors would like to thank the National Science Foundation (CHE-1707347) for support, and the Department of Biochemistry and Molecular Biology at UCR for ITC measurements.

REFERENCES

(1) Klose, R. J.; Zhang, Y., Regulation of histone methylation by demethylimination and demethylation. *Nat. Rev. Mol. Cell Biol.* **2007**, *8*, 307-318.

(2) Walsh, C T. Posttranslational modification of proteins: expanding nature's inventory. W. H. Freeman, **2005**, ISBN 9780974707730.

(3) Fierz, B.; Muir, T.W. Chromatin as an expansive canvas for chemical biology *Nat. Chem. Biol.* **2012**, *8*, 417-427.

(4) (a) Sabari, B.R.; Zhang, D.; Allis, C.D.; Zhao, Y. Metabolic regulation of gene expression through histone acylations *Nat. Rev. Mol. Cell. Biol.* **2017**, *18*, 90-101. (b) Tan, M.; Luo, H.; Lee, S.; Jin, F.; Yang, J.S.; Montellier, E.; Buchou, T.; Cheng, Z.; Rousseaux, S.; Rajagopal, N.; Lu, Z.; Ye, Z.; Zhu, Q.; Wysocka, J.; Ye, Y.; Khochbin, S.; Ren, B.; Zhao, Y. Identification of 67 histone marks and histone lysine crotonylation as a new type of histone modification *Cell* **2011**, *146*, 1015–1027. (c) Dai, L. Z.; Peng, C.; Montellier, E.; Lu, Z.; Chen, Y.; Ishii, H.; Debernardi, A.; Buchou, T.; Rousseaux, S.; Jin, F.; Sabari, B.R.; Deng, Z.; Allis, C.D.; Ren, B.; Khochbin, S.; Zhao, Y. Lysine 2-hydroxyisobutyrylation is a widely distributed active histone mark *Nat. Chem. Biol.* **2014**, *10*, 365–370.

(5) (a) Lachner, M.; O'Carroll, D.; Rea, S.; Mechtler, K.; Jenuwein, T. Methylation of histone H3 lysine 9 creates a binding site for HP1 proteins *Nature* **2001**, *410*, 116–120. (b) Rea, S.; Eisenhaber, F.; O'Carroll, D.; Strahl, B. D.; Sun, Z.-W.; Schmid, M.; Opravil, S.; Mechtler, K.; Ponting, C. P.; Allis, C. D.; Jenuwein, T. Regulation of chromatin structure by site-specific histone H3 methyltransferases Nature **2000**, *406*, 593–599.

(6) (a) Thompson, L.L.; Guppy, B.J.; Sawchuk, L.; Davie, J.R.; McManus, K.J. Regulation of chromatin structure via histone post-translational modification and the link to carcinogenesis *Cancer Metastasis Rev.* **2013**, *32*, 363-376. (b) Mowen, K. A.; David, M., Unconventional post-translational modifications in immunological signaling. *Nat. Immunol.* **2014**, *15*, 512-520. (c) Fleuren, E. D.; Zhang, L.; Wu, J.; Daly, R. J., The kinome 'at large' in cancer. *Nat. Rev. Cancer* **2016**, *16*, 83-98.

(7) (a) Zybailov, B.; Sun, Q.; van Wijk, K. J., Workflow for Large Scale Detection and Validation of Peptide Modifications by RPLC-LTQ-Orbitrap: Application to the Arabidopsis thaliana Leaf Proteome and an Online Modified Peptide Library *Anal. Chem.* **2009**, *81*, 8015-8024. (b) Monroe, M. E.; Tolic, N.; Jaitly, N.; Shaw, J. L.; Adkins, J. N.; Smith, R. D., VIPER: an advanced software package to support high-throughput LC-MS peptide identification *Bioinformatics* **2007**, *23*, 2021-2023.

(8) (a) Hattori, T.; Taft, J.M.; Swist, K.M.; Luo, H.; Witt, H.; Slattery, M.; Koide, A.; Ruthenburg, A.J.; Krajewski, K.; Strahl, B.D.; White, K.P.; Farnham, P.G.; Zhao, Y.; Koide, S. Recombinant antibodies to histone post-translational modifications *Nat. Methods* **2013**,*10*, 992-995. (b) Ting, A. Y.; Kain, K. H.; Klemke, R. L.; Tsien, R. Y., Genetically encoded fluorescent reporters of protein tyrosine kinase activities in living cells. *Proc. Natl. Acad. Sci. USA* **2001**, *98*, 15003–15008. (c) Hayashi-Takanaka, Y.; Yamagata, K.; Wakayama, T.; Stasevich, T.J.; Kainuma, T.; Tsurimoto, T.; Tachibana, M.; Shinkai, Y.; Kurumizaka, H.; Nozaki, N.; Kimura, H. Tracking epigenetic histone modifications in single cells using Fab-based live endogenous modification labeling *Nucleic Acids Res.* **2011**, *39*, 6475-6488.

(9) Bradbury, A.; Plückthun, A. Standardize antibodies used in research. *Nature* **2015**, *518*, 27-29.

(10) (a) Beaver, J.; Waters, M.L. Molecular Recognition of Lys and Arg Methylation *ACS Chem. Biol.* **2016**, *11*, 643–653. (b) Daze, K. D.; Hof, F., The Cation–π Interaction at Protein–Protein Interaction Interfaces: Developing and Learning from Synthetic Mimics of

Proteins That Bind Methylated Lysines. *Acc. Chem. Res.* **2013**, *46*, 937-945.

(11) Dsouza, R. N.; Hennig, A.; Nau, W. M., Supramolecular Tandem Enzyme Assays. *Chem.-Eur. J.* **2012**, *18*, 3444-3459.

(12) (a) Umali, A. P.; Anslyn, E.V. A general approach to differential sensing using synthetic molecular receptors *Curr. Opin. Chem. Biol.* **2010**, *14*, 685–692. (b) You, L.; Zha, D.; Anslyn, E. V., Recent Advances in Supramolecular Analytical Chemistry Using Optical Sensing. *Chem. Rev.* **2015**, *115*, 7840-7892.

(13) (a) Minaker, S.A.; Daze, K.D.; Ma, M.C.F.; Hof, F. Antibody-Free Reading of the Histone Code Using a Simple Chemical Sensor Array *J. Am. Chem. Soc.* **2012**, *134*, 11674–11680. (b) Daze, K. D.; Pinter, T.; Beshara, C. S.; Ibraheem, A.; Minaker, S. A.; Ma, M. C. F.; Courtemanche, R. J. M.; Campbell, R. E.; Hof, F., Supramolecular hosts that recognize methyllysines and disrupt the interaction between a modified histone tail and its epigenetic reader protein. *Chem. Sci.* **2012**, *3*, 2695-2699.

(14) (a) Peacor, B. C.; Ramsay, C. M.; Waters, M. L., Fluorogenic sensor platform for the histone code using receptors from dynamic combinatorial libraries. *Chem. Sci.* **2017**, *8*, 1422-1428. (b) James, L. I.; Beaver, J. E.; Rice, N. W.; Waters, M. L., A Synthetic Receptor for Asymmetric Dimethyl Arginine. *J. Am. Chem. Soc.* **2013**, *135*, 6450-6455.

(15) (a) Barrow, S. J.; Kasera, S.; Rowland, M. J.; del Barrio, J.; Scherman, O. A., Cucurbituril-Based Molecular Recognition. *Chem. Rev.* **2015**, *115*, 12320-12406. (b) Guagnini, F.; Antoniuk, P.M.; Rennie, M.L.; O'Byrne, P.; Khan, A. R.; Pinalli, R.; Dalcanale, E.; Crowley, P.B. Cucurbit[7]uril-Dimethyllysine Recognition in a Model Protein. *Angew. Chem., Int. Ed.* **2018**, *57*, 7126-7130. (c) Heitmann, L. M.; Taylor, A. B.; Hart, P. J.; Urbach, A. R., Sequence-Specific Recognition and Cooperative Dimerization of N-Terminal Aromatic Peptides in Aqueous Solution by a Synthetic Host. *J. Am. Chem. Soc.* **2006**, *128*, 12574-12581.

(16) Hargrove, A. E.; Nieto, S.; Zhang, T.; Sessler, J. L.; Anslyn, E. V., Artificial Receptors for the Recognition of Phosphorylated Molecules. *Chem. Rev.* **2011**, *111*, 6603-6782.

(17) (a) Ojida, A.; Mito-oka, Y.; Inoue, M.-A.; Hamachi, I., First Artificial Receptors and Chemosensors toward Phosphorylated Peptide in Aqueous Solution. *J. Am. Chem. Soc.* **2002**, *124*, 6256-6258. (b) Breslow, R.; Yang, Z.; Ching, R.; Trojandt, G.; Odobel, F., Sequence Selective Binding of Peptides by Artificial Receptors in Aqueous Solution. *J. Am. Chem. Soc.* **1998**, *120*, 3536-3537.

(18) (a) Conway, J. H.; Fiedler, D., An Affinity Reagent for the Recognition of Pyrophosphorylated Peptides. *Angew. Chem. Int. Ed.* **2015**, *54*, 3941-3945. (b) Minami, T.; Liu, Y.; Akdeniz, A.; Koutnik, P.; Esipenko, N. A.; Nishiyabu, R.; Kubo, Y.; Anzenbacher, P., Intramolecular Indicator Displacement Assay for Anions: Supramolecular Sensor for Glyphosate. *J. Am. Chem. Soc.* **2014**, *136*, 11396-11401.

(19) (a) Zhang, T.; Edwards, N. Y.; Bonizzoni, M.; Anslyn, E. V., The Use of Differential Receptors to Pattern Peptide Phosphorylation. *J. Am. Chem. Soc.* **2009**, *131*, 11976-11984. (b) Wright, A.T.; Anslyn, E.V.; McDevitt, J.T. A differential array of metalated synthetic receptors for the analysis of tripeptide mixtures *J. Am. Chem. Soc.* **2005**, *127*, 17405-17411.

(20) (a) Hennig, A.; Bakirci, H.; Nau, W.M. Label-free continuous enzyme assays with macrocycle-fluorescent dye complexes *Nat. Methods* **2007**, *4*, 629-632. (b) Nau, W. M.; Ghale, G.; Hennig, A.; Bakirci, H.; Bailey, D. M. Substrate-Selective Supramolecular Tandem Assays: Monitoring Enzyme Inhibition of Arginase and Diamine Oxidase by Fluorescent Dye Displacement from Calixarene and Cucurbituril Macrocycles *J. Am. Chem. Soc.* **2009**, *131*, 11558–11570. (c) Florea, M.; Kudithipudi, S.; Rei, A.; González-Álvarez, M. J.; Jeltsch, A.; Nau, W. M. A Fluorescence-Based Supramolecular Tandem Assay for Monitoring Lysine Methyltransferase Activity in Homogeneous Solution *Chem.-Eur. J.* **2012**, *18*, 3521-3528.

(21) (a) Lawrence, D. S.; Wang, Q., Seeing is believing: peptide-based fluorescent sensors of protein tyrosine kinase activity. *Chembiochem* **2007**, *8*, 373-378. (b) Shults, M. D.; Imperiali, B., Versatile Fluorescence Probes of Protein Kinase Activity. *J. Am. Chem. Soc.* **2003**, *125*, 14248-14249. (c) Chen, C.-A.; Yeh, R.-H.; Lawrence, D. S., Design and Synthesis of a Fluorescent Reporter of Protein Kinase Activity. *J. Am. Chem. Soc.* **2002**, *124*, 3840-3841. (d) Sahoo, H.; Hennig, A.; Florea, M.; Roth, D.; Enderle, T.; Nau, W. M., Single-Label Kinase and Phosphatase Assays for Tyrosine Phosphorylation Using Nanosecond Time-Resolved Fluorescence Detection. *J. Am. Chem. Soc.* **2007**, *129*, 15927-15934. (e) Zamora-Olivares, D.; Kaoud, T. S.; Dalby, K. N.; Anslyn, E. V., In-Situ Generation of Differential Sensors that Fingerprint Kinases and the Cellular Response to Their Expression. *J. Am. Chem. Soc.* **2013**, *135*, 14814-14820. (f) Anai, T.; Nakata, E.; Koshi, Y.; Ojida, A.; Hamachi, I., Design of a Hybrid Biosensor for Enhanced Phosphopeptide Recognition Based on a Phosphoprotein Binding Domain Coupled with a Fluorescent Chemosensor. *J. Am. Chem. Soc.* **2007**, *129*, 6232-6239. (g) Wang, Q.; Lawrence, D. S., Phosphorylation-Driven Protein–Protein Interactions: A Protein Kinase Sensing System. *J. Am. Chem. Soc.* **2005**, *127* (21), 7684-7685.

(22) (a) Peng, S.; Barba-Bon, A.; Pan, Y.-C.; Nau, W. M.; Guo, D.-S.; Hennig, A. Phosphorylation-Responsive Membrane Transport of Peptides. *Angew. Chem. Int. Ed.* **2017**, **56**, 15742 –15745. (b) Florea, M.; Nau, W.M. Implementation of anion-receptor macrocycles in supramolecular tandem assays for enzymes involving nucleotides as substrates, products, and cofactors. *Org. Biomol. Chem.* **2010**, *8*, 1033-1039.

(23) (a) Hooley, R.J.; van Anda, H.J.; Rebek, J., Jr. Extraction Of Hydrophobic Species Into A Water-Soluble Synthetic Receptor *J. Am. Chem. Soc.* **2007**, *129*, 13464-13473. (b) Biros, S. M.; Ullrich, E. C.; Hof, F.; Trembleau, L.; Rebek, J., Kinetically Stable Complexes in Water: The Role of Hydration and Hydrophobicity. *J. Am. Chem. Soc.* **2004**, *126*, 2870-2876.

(24) (a) Liu, Y.; Perez, L.; Mettry, M.; Easley, C. J.; Hooley, R. J.; Zhong, W., Self-Aggregating Deep Cavitand Acts as a Fluorescence Displacement Sensor for Lysine Methylation. *J. Am. Chem. Soc.* **2016**, *138*, 10746-10749. (b) Liu, Y.; Perez, L.; Mettry, M.; Gill, A. D.; Byers, S. R.; Easley, C. J.; Bardeen, C. J.; Zhong, W.; Hooley, R. J., Site selective reading of epigenetic markers by a dual-mode synthetic receptor array. *Chem. Sci.* **2017**, *8*, 3960-3970. (c) Liu, Y.; Perez, L.; Gill, A. D.; Mettry, M.; Li, L.; Wang, Y.; Hooley, R. J.; Zhong, W., Site-Selective Sensing of Histone Methylation Enzyme Activity *via* an Arrayed Supramolecular Tandem Assay. *J. Am. Chem. Soc.* **2017**, *139*, 10964-10967.

(25) Liu, Y.; Mettry, M.; Gill, A. D.; Perez, L.; Zhong, W.; Hooley, R. J., Selective Heavy Element Sensing with a Simple Host–Guest Fluorescent Array. *Anal. Chem.* **2017**, *89*, 11113-11121.

(26) Jurs, P. C.; Bakken, G. A.; McClelland, H. E., Computational Methods for the Analysis of Chemical Sensor Array Data from Volatile Analytes. *Chem. Rev.* **2000**, *100*, 2649-2678.

(27) de la Peña, A. M.; Salanas, F.; Gómez, M. J.; Acedo, M. I.; Peña, M. S. *J. Inclus. Phenom. Mol. Rec. Chem*. **1993**, *15*, 131-143.

(28) Easley, C.J.; Mettry, M.; Moses, E.M.; Hooley, R.J.; Bardeen, C.J. Boosting the Heavy Atom Effect by Cavitand Encapsulation: Room Temperature Phosphorescence of Pyrene in the Presence of Oxygen. *J. Phys. Chem. A.* **2018**, *122*, 6578-6584.

(29) Hulme, E.C.; Birdsall, N.J.M. Strategy and Tactics in Receptor-Binding Studies. In *Receptor–Ligand Interactions: A Practical Approach*, Hulme, E.C. ed., Oxford University Press, 1992, pp 63–176.

(30) (a) Tonks N. K., Protein tyrosine phosphatases – from housekeeping enzymes to master regulators of signal transduction. *FEBS J.* **2013**, *280*, 346-378. (b) Bamborough, P., System-based drug discovery within the human kinome. *Expert Opin. Drug Discov.* **2012**, *7*, 1053-1070.

(31) Pearce, L. R.; Komander, D.; Alessi, D. R. The nuts and bolts of AGC protein kinases. *Nat. Rev. Mol. Cell Biol.* **2010**, *11*, 9-22.

(32) (a) Zhang, K.; Lin, W.; Latham, J. A.; Riefler, G. M.; Schumacher, J. M.; Chan, C.; Tatchell, K.; Hawke, D. H.; Kobayashi, R.; Dent, S. Y. R. The Set1 Methyltransferase Opposes Ipl1 Aurora Kinase Functions in Chromosome Segregation. *Cell*, **2005**, *122*, 723–734. (b) Rea, S.; Eisenhaber, F.; O'Carroll, D.; Strahl, B.D.; Sun, Z.-W.;

Schmid, M.; Opravil, S.; Mechtler, K.; Ponting, C.P.; Allis, C.D.; Jenuwein, T. Regulation of chromatin structure by site-specific histone H3 methyltransferases. *Nature* **2000**, *406*, 593-599.

(33) Kumar, R.; Deivendran, S.; Santhoshkumar, T. R.; Pillai, M. R. Signaling coupled epigenomic regulation of gene expression. *Oncogene*, **2017**, *36*, 5917–5926.

TOC Entry:

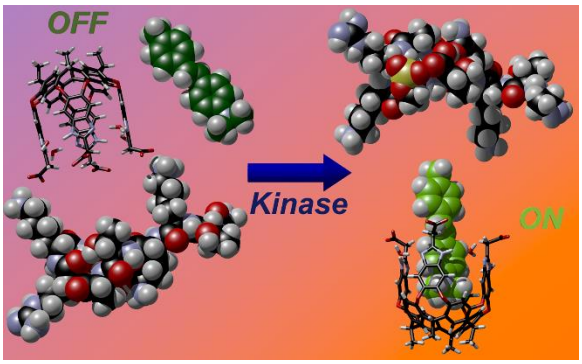

Selective Sensing of Phosphorylated Peptides and Monitoring Kinase and Phosphatase Activity with a Supramolecular Tandem Assay

Yang Liu,[2] Jiwon Lee,[1] Lizeth Perez,[1] Adam D. Gill,[3] Richard J. Hooley[1,3] and Wenwan Zhong[1,2]**

[1]Department of Chemistry; [2]Environmental Toxicology Program; [3]Department of Biochemistry and Molecular Biology; University of California-Riverside, Riverside, CA 92521, U.S.A.

richard.hooley@ucr.edu; wenwan.zhong@ucr.edu

Supporting Information

Table of Contents:

1. Supporting Figures

I) Turn-on fluorescence of DSMI upon binding to cavitand

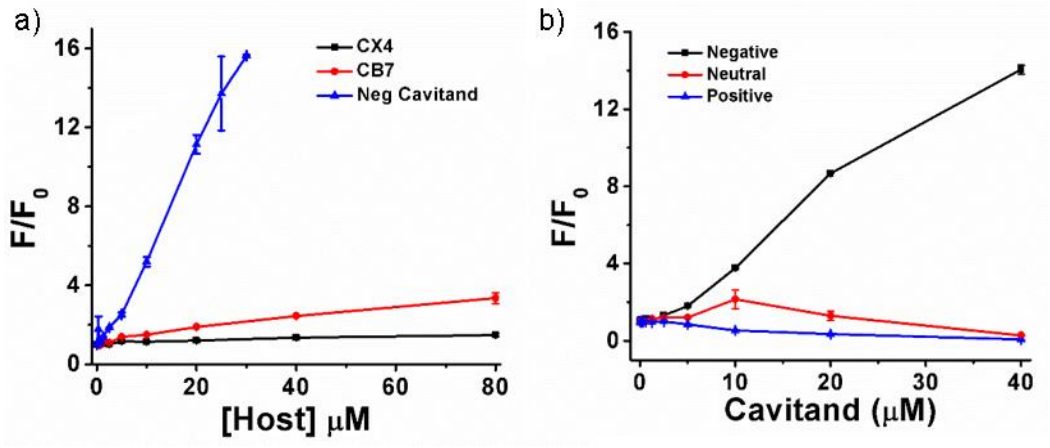

Figure S-1. Fluorescence enhancement of guest **3** with different hosts – cavitand **1**, tetrasulfonatocalix[4]arene (CX4), and cucurbit[7]uril (CB7) (a) and different cavitands (b)[2]. [**3**] = 1.5 μM, Phosphate buffer, 100 mM, pH =7.4.

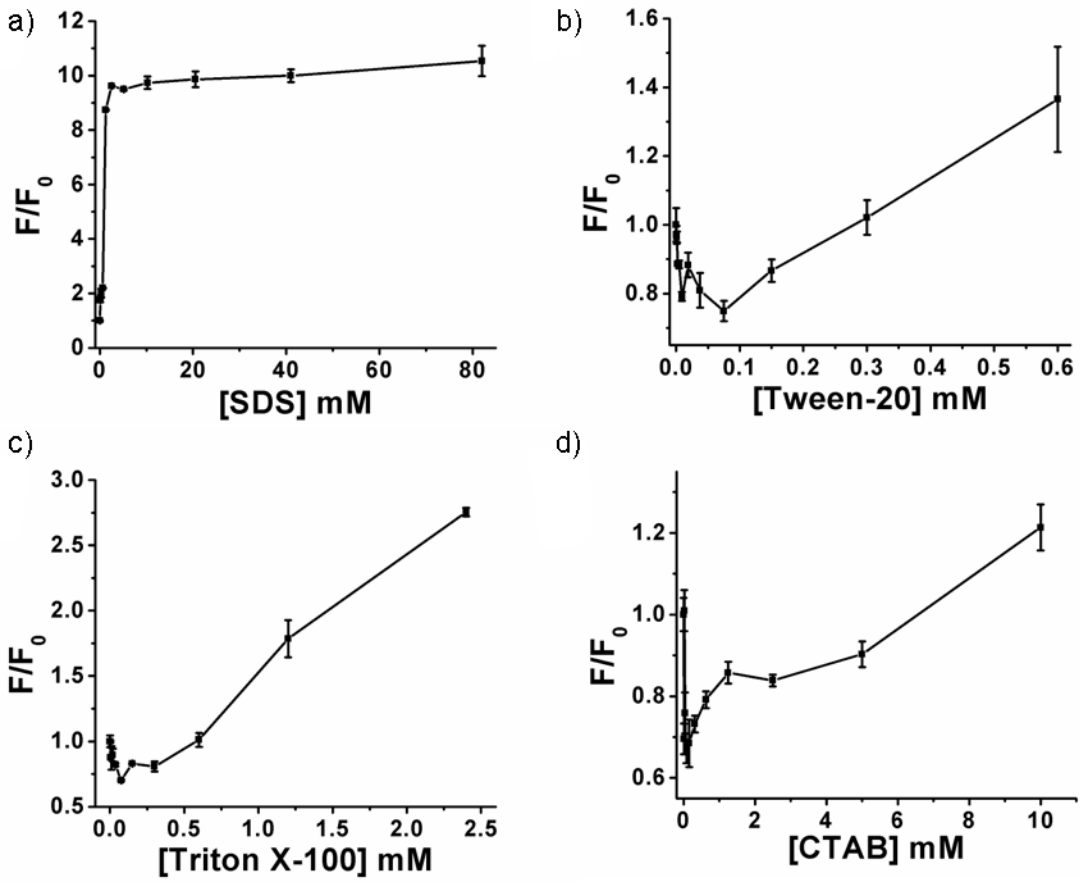

Figure S-2. a) Fluorescence enhancement of guest **3** with different surfactants. a) SDS, b) Tween-20, c) Triton X-100, d) CTAB. [**3**] = 1.5 μM, 100 mM Phosphate at pH 7.4.

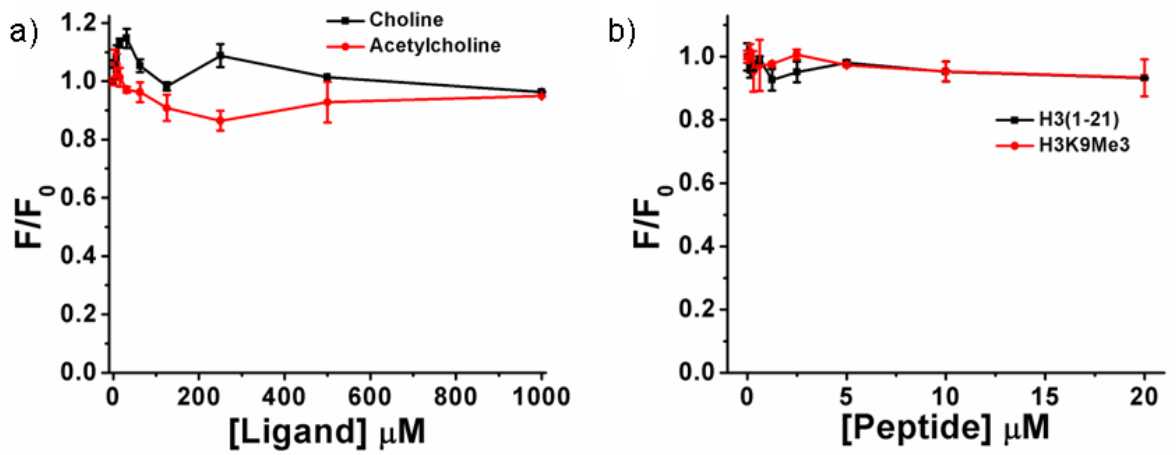

Figure S-3. a) Competition of small molecules (a) and peptides (b) with **3** for binding to **1**. [**3**] = 1.5 μM, [**1**] = 20 μM, 20 mM Tris-HCl at pH 7.4.

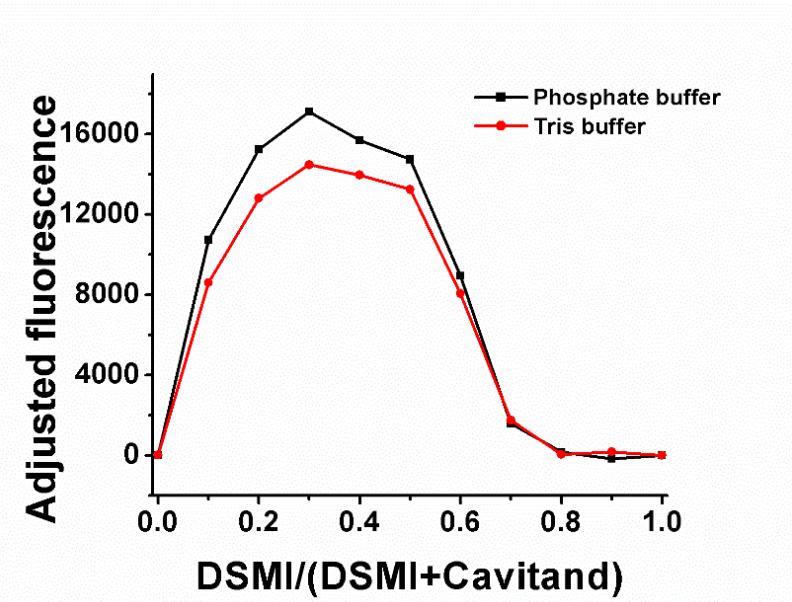

Figure S-4. Job plot for the binding between **3** and **1** in 100 mM Phosphate or 20 mM Tris buffer, both at pH 7.4. Adjusted fluorescence = F – [DSMI ratio] * $F_{[DSMI\ ratio = 1]}$

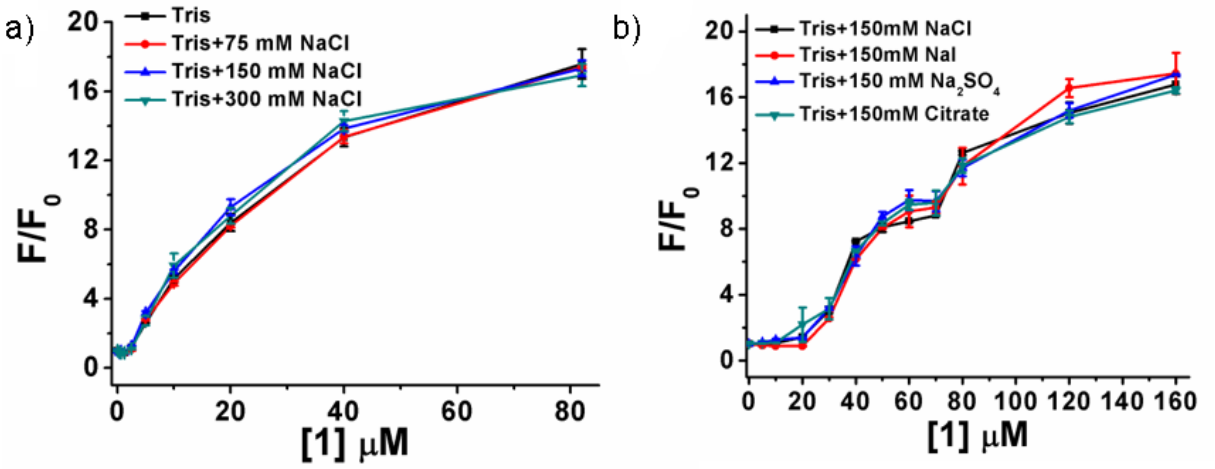

Figure S-5. Influence of ion strength and anion type on fluorescence enhancement of **1•3**. a) different concentrations of NaCl, [**1**] = 20 μM, [**3**] = 1.5 μM, 20 mM Tris, pH 7.4; b) different anion types, [**1**] = 40 μM, [**3**] = 40 μM, 20 mM Tris, pH 7.4.

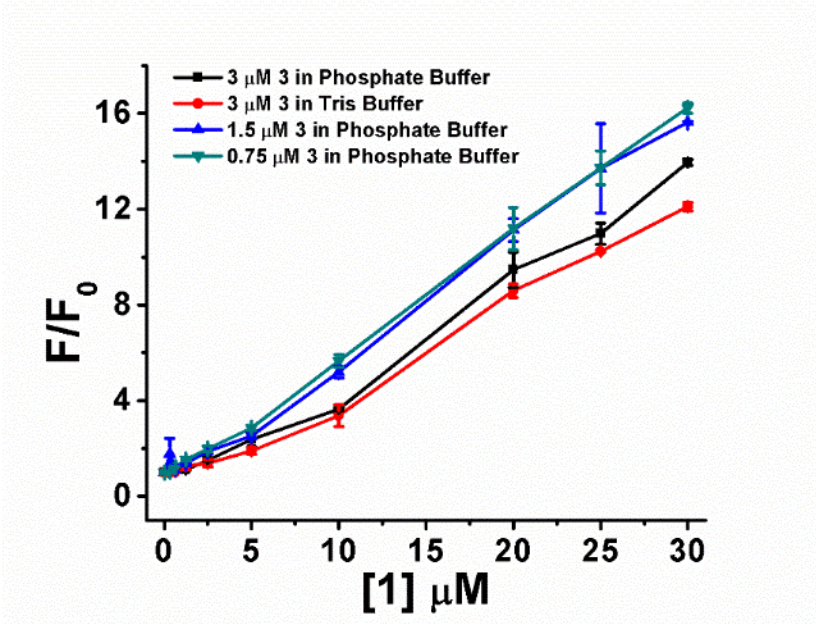

Figure S-6. Influence of phosphate anion on fluorescence enhancement of **1•3** in either 50 mM Phosphate or 50 mM Tris, both at pH 7.4.

II). Fluorescence responses of the cavitand-based sensors for various PTMs

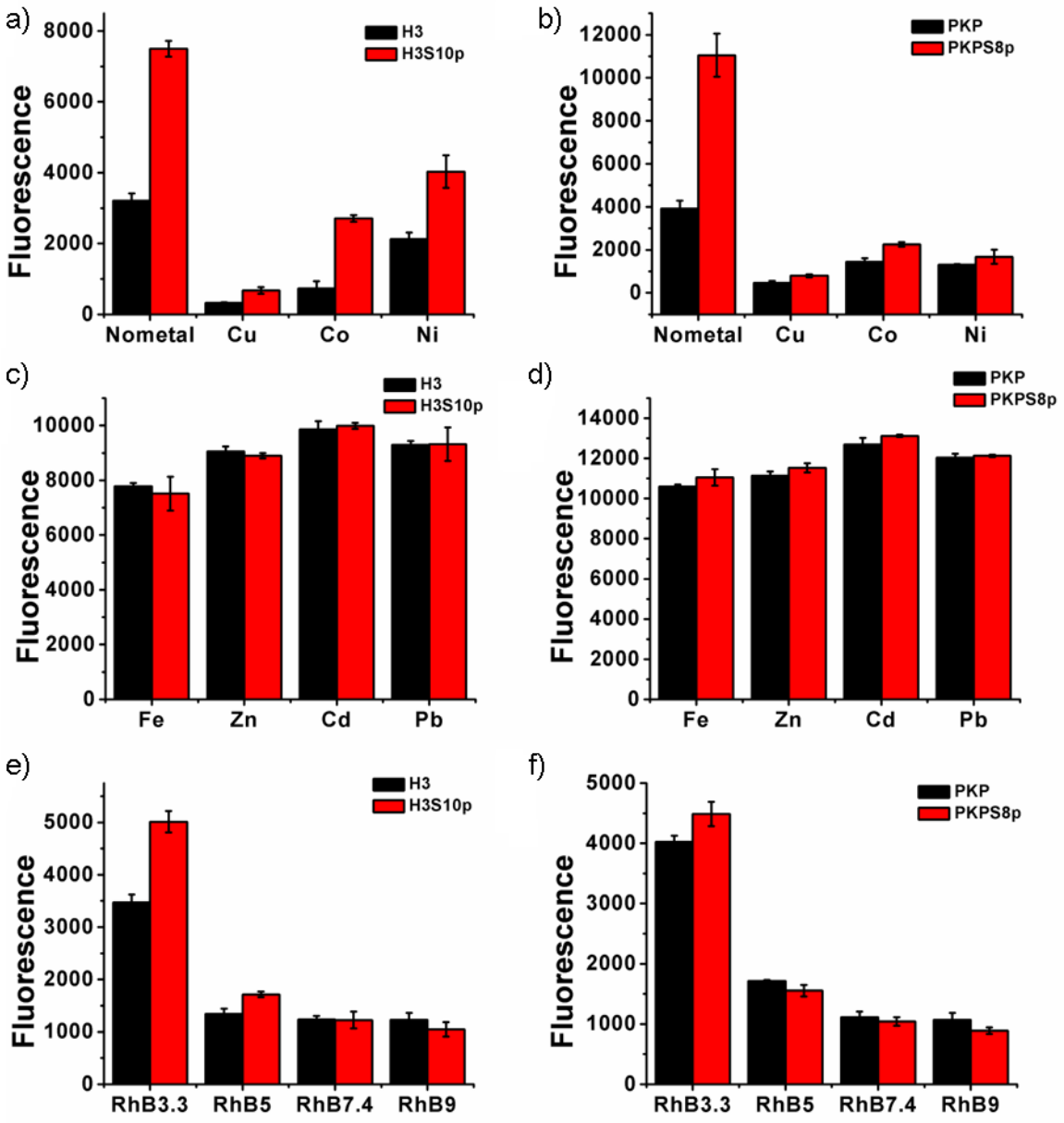

Figure S-7. Raw fluorescence plots for the data shown in Figures 2a and 2b. [peptide] = 10 μM. **1•3•M^{2+}**: [**1**] = 20 μM, [**3**] = 1.5 μM, [M^{2+}] = 10 μM, 20 mM Tris, pH 7.4. **1•2**: [**1**] = 3 μM, [**2**] = 4 μM, [M^{2+}] = 10 μM. RhB3.3, 5, 7.4, and 9 correspond to guest **2 (RhB)** in buffer at pH 3.3, 5, 7.4, or 9.

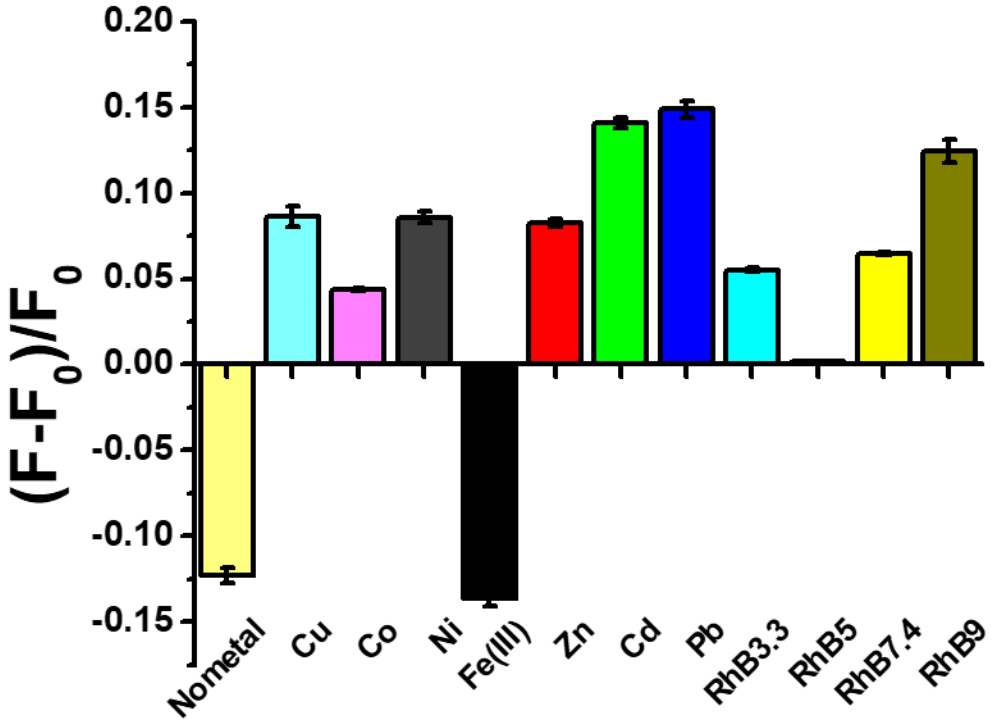

Figure S-8. Relative fluorescence response of H3K9Ac with different sensor array elements. F_0 = fluorescence of H3 peptide, F = fluorescence of H3K9Ac peptide; [peptide] = 10 μM. **1•3•M^{2+}**: [**1**] = 20 μM, [**3**] = 1.5 μM, [**M^{2+}**] = 10 μM, 20 mM Tris, pH 7.4. **1•2**: [**1**] = 3 μM, [**2 (RhB)**] = 4 μM, [**M^{2+}**] = 10 μM. RhB3.3, 5, 7.4, and 9 correspond to guest **2 (RhB)** in buffer at pH 3.3, 5, 7.4, or 9.

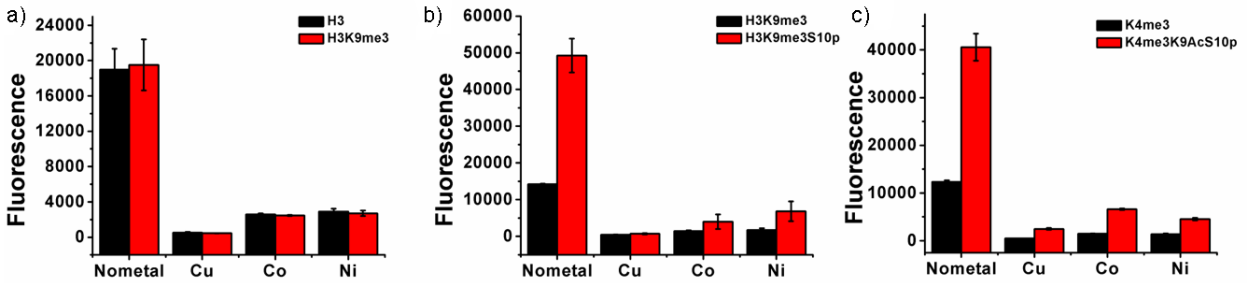

Figure S-9. Fluorescence response of **1•3•M^{2+}** with peptide phosphorylation in the presence of other PTMs. (a) methylation; b) methylation plus phosphorylation; c) methylation plus acetylation plus phosphorylation. [peptide] = 10 μM. **1•3•M^{2+}**: [**1**] = 20 μM, [**3**] = 1.5 μM, [**M^{2+}**] = 10 μM, 20 mM Tris, pH 7.4.

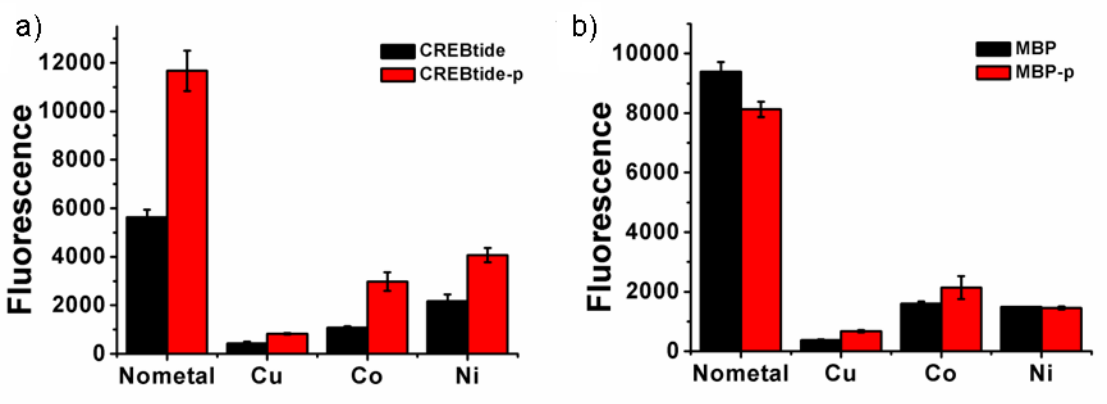

Figure S-10. Fluorescence response of **1•3•M**$^{2+}$ with phosphorylated peptide. (a) CREBtide; b) MBP. [peptide] = 10 μM. **1•3•M**$^{2+}$: [**1**] = 20 μM, [**3**] = 1.5 μM, [**M**$^{2+}$] = 10 μM, 20 mM Tris, pH 7.4.

III). Isothermal Calorimetry analysis of cavitand:peptide interactions

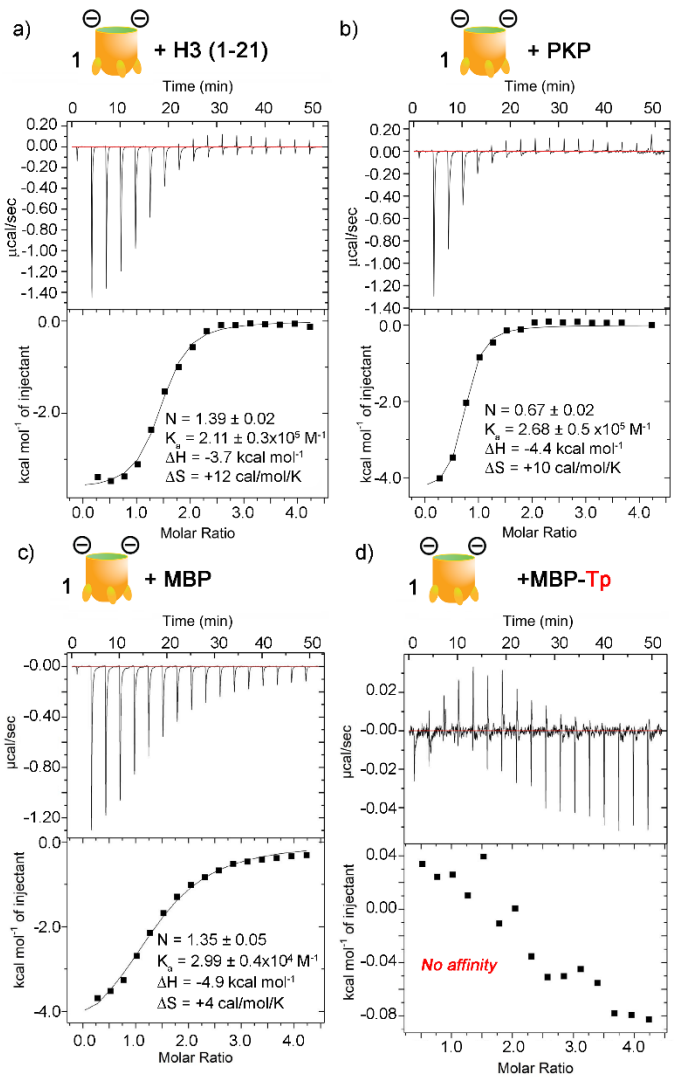

Figure S-11. ITC data for the addition of aliquots of 2.43 µL 2 mM of cavitand **1** to a) H3 (1-21), b) protein kinase A substrate PKP (GRTGRRNSI); c) MBP (Biotin-APRTPGGRR) and d) MBP-Tp (Biotin-APR-pT-PGGRR). [peptide] = 100 µM in 20 mM Tris buffer at pH 7.4.

IV). *In situ* monitoring of peptide phosphorylation and dephosphorylation

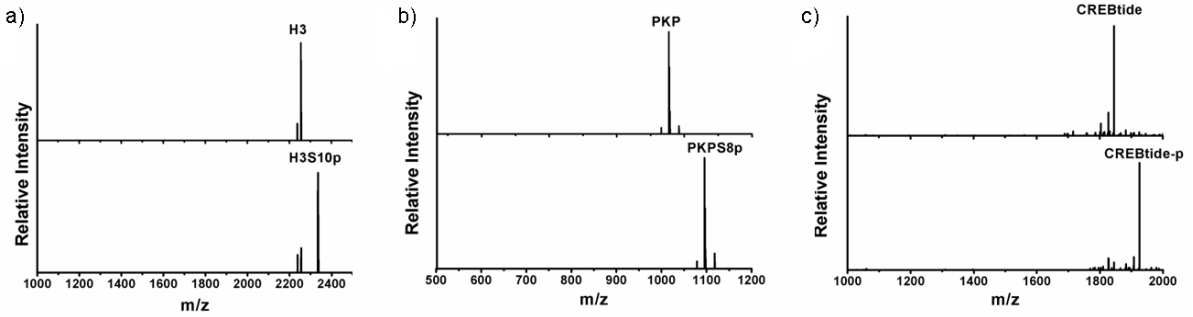

Figure S-12. MALDI confirmation of a) H3 and b) PKP phosphorylation by PKA, as well as c) CREBtide-p dephosphorylation by alkaline phosphatase. Reaction conditions the same as in Fig. S14 and S18.

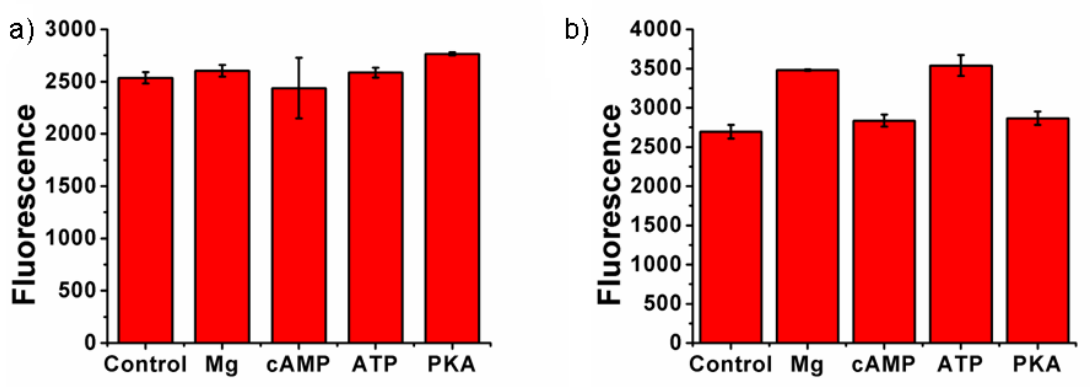

Figure S-13. Phosphorylation reaction additives' influence on fluorescence enhancement of **1•3**. a) 1 mM Mg^{2+}, 5 μM cAMP, 50 μM ATP and 0.01mg/mL PKA. b) 10 mM Mg^{2+}, 50 μM cAMP, 500 μM ATP, 0.1 mg/mL PKA.

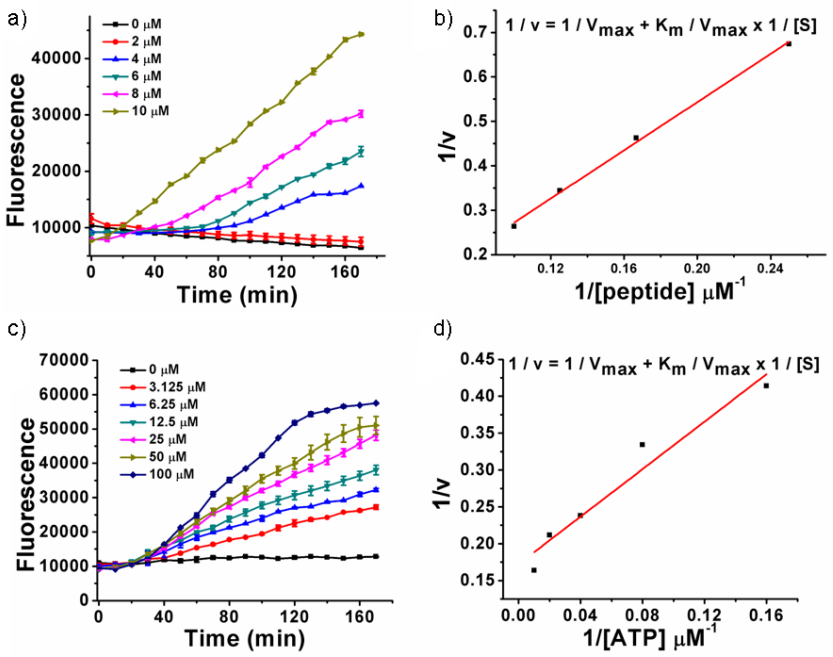

Figure S-14. Kinetic study on PKA activity and Michaelis–Menten constant K_m calculation using the Lineweaver-Burke plot with varying concentrations of H3 peptide (a, b) and ATP(c,d). Enzyme reaction solution: Mg^{2+} = 1 mM, ATP = 20 μM (for a, b), cAMP = 5 μM, H3 peptide = 10 μM (for c, d) and PKA = 0.01 mg/mL, 20 mM Tris buffer at pH = 7.4.

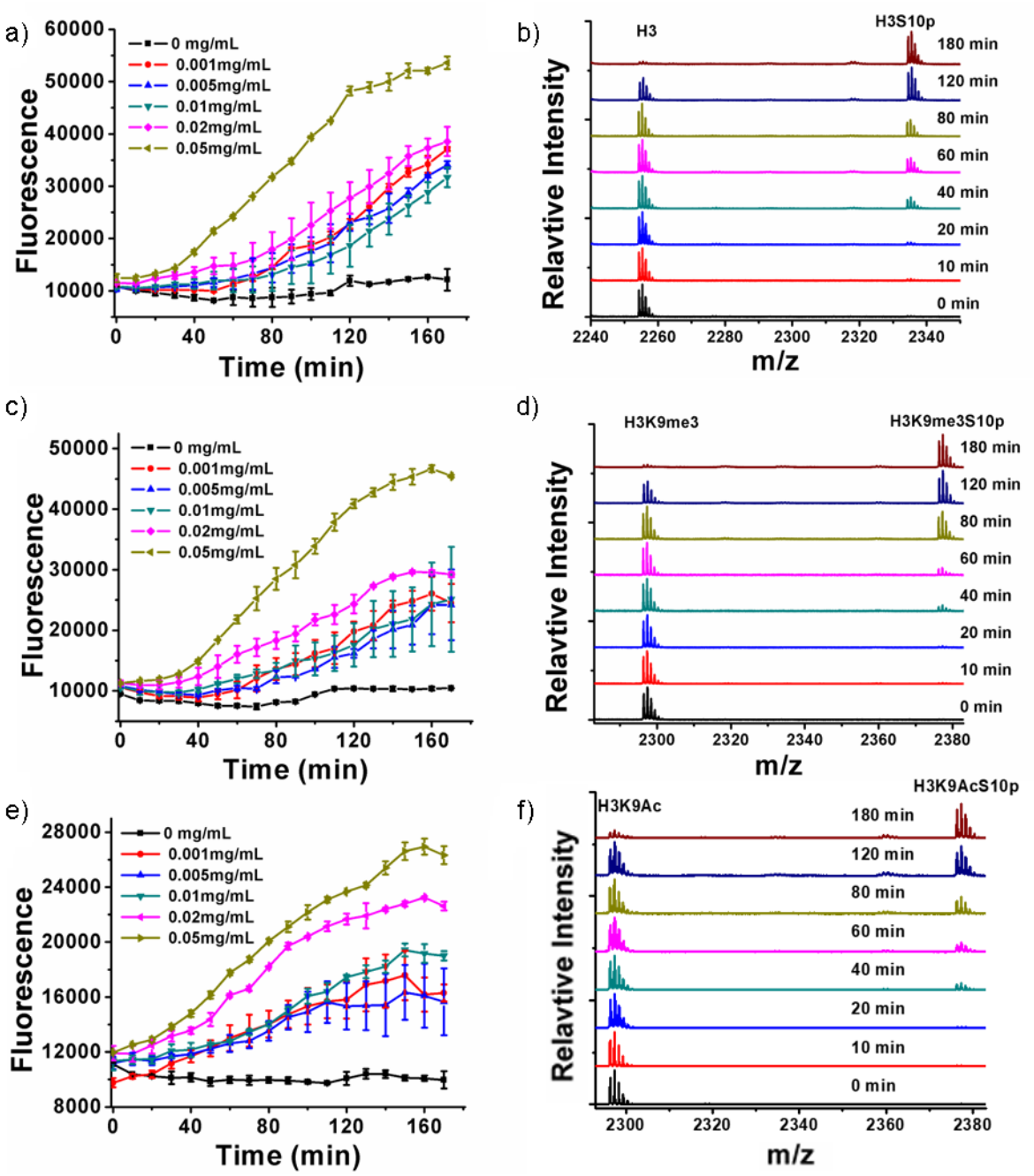

Figure S-15. Kinetic study on PKA activity with H3, H3K9me$_3$ and H3K9Ac peptide as substrates. a) H3 peptide as substrates with various concentrations of PKA (0-0.05 mg/mL), b) MALDI verification of figure a; c) H3K9me$_3$ peptide as substrates with various concentrations of PKA (0-0.05 mg/mL), d) MALDI verification of figure c. e) H3K9Ac peptide as substrates with various concentrations of PKA (0-0.05 mg/mL), f) MALDI verification of figure e. PKA Enzyme reaction solution: Mg^{2+} = 1 mM, ATP = 20 μM, cAMP = 5 μM, H3 peptide = 10 μM, 20 mM Tris buffer, pH = 7.4.

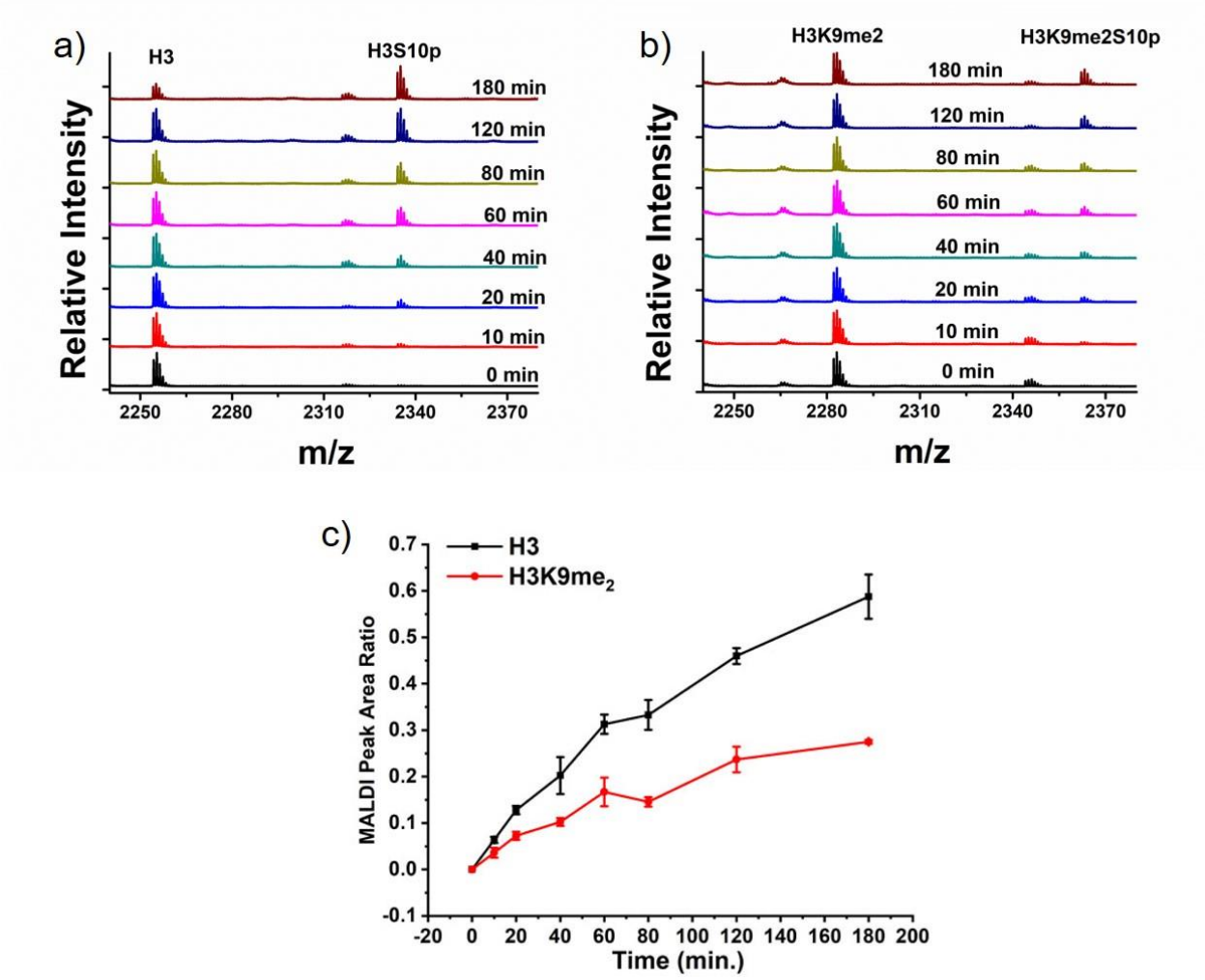

Figure S-16. MALDI verification of fluorescence assay results shown in Fig. 7b, which compared the kinetics of phosphorylation on a) H3 (1-21) and b) H3K9me$_2$ by the methylation-selective Aurora B Kinase, with the averaged area ratios of the phosphorylated product over the sum of phosphorylated product and non-phosphorylated substrate plotted against reaction duration displayed in c). Enzyme reaction conditions: 0.005 μg/μl enzyme, 10 μM peptide substrate, 0.1 mM Mg^{2+}, 20 μM ATP, 20 mM Tris buffer at pH = 7.4.

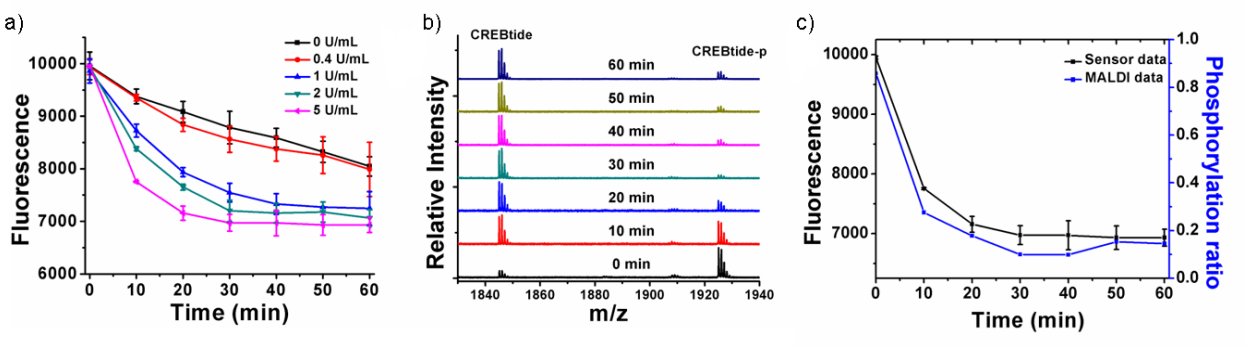

Figure S-17. Kinetic study on alkaline phosphatase activity with CREBTide-Yp substrate. a) Fluorescence response over time with various concentrations of alkaline phosphatase (0-5 U/mL), b) MALDI verification of the data in Figure S-17a; c) Matching of fluorescence data with MALDI data. Alkaline phosphatase enzyme reaction solution: [CREBTide-Yp] = 10 μM, Tris buffer, 20 mM, pH = 7.4.

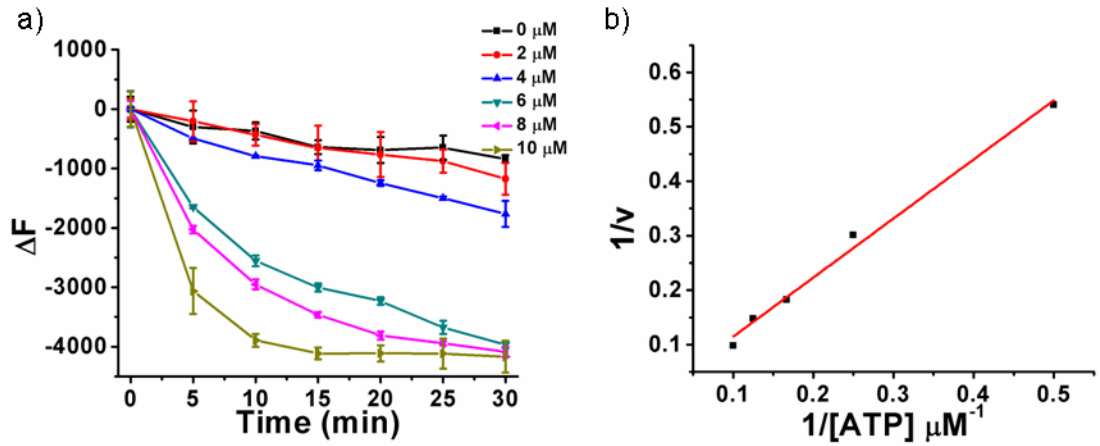

Figure S-18. Kinetic study on alkaline phosphatase activity and Michaelis–Menten constant K_m calculation using the Lineweaver-Burke plot with varying concentrations of CREBTibe-Yp. Alkaline phosphatase enzyme reaction solution: alkaline phosphatase = 5 U/mL, 20 mM Tris, pH = 7.4.